Chapter 5

Uncovering SUMOylation Dynamics during Cell-Cycle Progression Reveals FoxM1 as a Key Mitotic SUMO Target Protein

Joost Schimmel[1*], Karolin Eifler[1*], Jón Otti Sigurðsson[2*], Sabine A.G. Cuijpers[1], Ivo A. Hendriks[1], Matty Verlaan-de Vries[1], Christian D. Kelstrup[2], Chiara Francavilla[2], Rene´ H. Medema[3], Jesper V. Olsen[2], and Alfred C.O. Vertegaal[1]

[1]Department of Molecular Cell Biology, Leiden University Medical Center, Albinusdreef 2, 2333 ZA Leiden, the Netherlands
[2]Novo Nordisk Foundation Center for Protein Research, Faculty of Health and Medical Sciences, University of Copenhagen, Blegdamsvej 3B, 2200 Copenhagen, Denmark
[3]Department of Cell Biology, Netherlands Cancer Institute, Plesmanlaan 121, 1066 CX Amsterdam, the Netherlands
[*]These authors contributed equally to this work

Chapter 5 has been published in Molecular Cell

Mol Cell. 2014 Mar 20;53(6):1053-66. doi: 10.1016/j.molcel.2014.02.001.
Supplementary Tables are available online.

ABSTRACT

Loss of SUMO modification in mice causes genomic instability due to the missegregation of chromosomes. Currently, little is known about the identity of relevant SUMO target proteins that are involved in this process and about global SUMOylation dynamics during cell cycle progression. We performed a large-scale quantitative proteomics screen to address this and identified 593 proteins to be SUMO-2 modified, including the Forkhead transcription factor FoxM1, a key regulator of cell cycle progression and chromosome segregation. SUMOylation of FoxM1 peaks during G2 and M phase, when FoxM1 transcriptional activity is required. We found that a SUMOylation deficient FoxM1 mutant was less active compared to wild-type FoxM1, implicating that SUMOylation of the protein enhances its transcriptional activity. Mechanistically, SUMOylation blocks the dimerization of FoxM1, thereby relieving FoxM1 autorepression. Cells deficient for FoxM1 SUMOylation showed increased levels of polyploidy. Our findings contribute to understanding the role of SUMOylation during cell cycle progression.

INTRODUCTION

Cell cycle progression is extensively controlled via complex networks of reversible post-translational modifications (PTMs), including small chemical modifications like phosphorylation and modifications by ubiquitin and small ubiquitin-like proteins [1-3]. Deregulation of these signaling cascades can result in uncontrolled cell cycle progression, causing genome instability and cancer [4-6]. Cell cycle signal transducers represent major anti-cancer drug targets that are exploited to halt cell cycle progression in tumor cells [7].

More recently, mass spectrometry (MS)-based proteomics has enabled global analyses of different post-translational modification networks, including phosphorylation, ubiquitylation and lysine acetylation [8]. Interestingly, nuclear proteins and proteins involved in regulating metabolic processes showed significant cell cycle dynamics with notably high phosphorylation site occupancy in mitosis [9]. Initial studies on the small ubiquitin-like modifier (SUMO) system revealed a key role for this modification in cell cycle progression [10-13]. A failure to conjugate the single SUMO form in *S. cerevisiae*, Smt3, to target proteins due to a deletion of Ubc9 resulted in a G2/M block [14]. Conversely, a failure to remove Smt3 from a subset of target proteins due to a deletion of the SUMO protease Ulp1 in *S. cerevisiae* also resulted in a G2/M block [15] and Ulp2 is essential for spindle dynamics and cell cycle progression [16]. Mice deficient for Ubc9 failed to progress through embryonic development and died at the early post-implantation stage due to DNA hypocondensation and genome instability [17].

Multiple SUMO target proteins were identified that play key roles during cell cycle progression including the trimeric replication clamp PCNA [18, 19], DNA topoisomerase IIα [20], CENP-E (Zhang et al., 2008), CENP-I [21] and the chromosomal passenger complex subunit Borealin [22]. Despite these interesting findings, we are lacking global insight in the regulation of cell cycle progression via SUMOylation. To address this, we have optimized the biochemical purification of SUMO target proteins and used a SILAC approach [23] to compare SUMOylation levels of these targets at different cell cycle stages. Follow-up experiments revealed that SUMOylation was needed for full transcriptional activation of the Forkhead box transcription factor FoxM1 and for counteracting polyploidy. Mechanistically, SUMOylation counteracts auto-repression of FoxM1.

RESULTS

Knockdown of UBA2 and Ubc9 in HeLa cells leads to decreased cell proliferation

To study the role of SUMOylation in cell cycle progression in a mammalian system, we infected HeLa and U2OS cells with lentiviruses encoding shRNA against UBA2, Ubc9 or for a non-coding control shRNA. Western blot analysis confirmed that UBA2 and Ubc9 protein levels as well as the amount of SUMO conjugates were

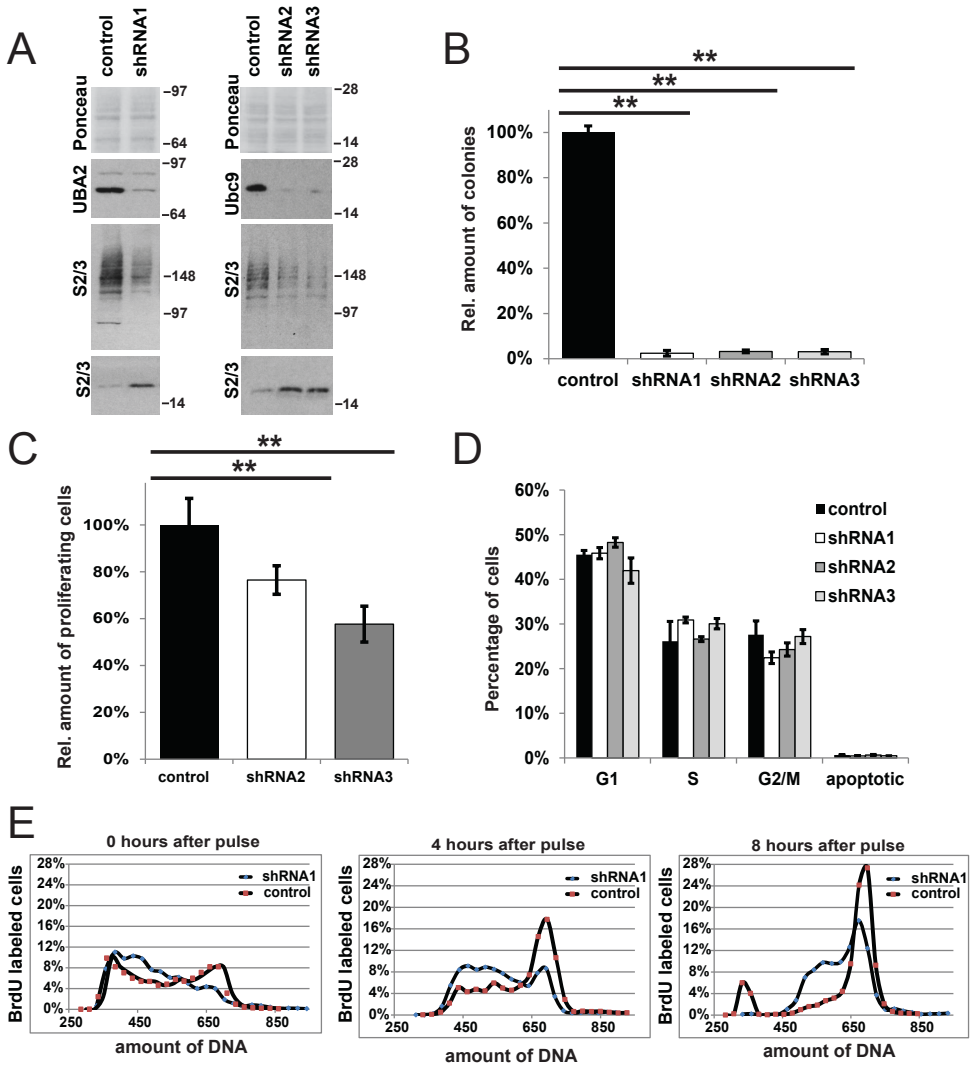

Figure 1. SUMOylation is required for cell proliferation

A) HeLa cells were infected with lentiviruses expressing an shRNA against UBA2 (shRNA1) and two different shRNAs against Ubc9 (shRNA2 and shRNA3), or with a control virus respectively. A decrease in UBA2 and Ubc9 expression and SUMO conjugation levels and an increase in free SUMO was confirmed by immunoblotting four days after virus infection using antibodies against UBA2, Ubc9 and SUMO-2/3.

B) Colony formation was determined nine days after infection by staining with Giemsa solution and counting colonies using the ImageJ Version 1.47v software. The values were normalized to the control. Error bars represent the standard deviation from the average obtained from three independent experiments. ** $p < 0.001$.

C) The proliferation rate of cells treated with Ubc9 knockdown virus was compared to cells treated

reduced but not abrogated after virus infection, whereas the pool of free SUMO was increased (**Figure 1A**). Colony formation of cells treated with UBA2 and Ubc9 knockdown viruses was compared to the control nine days after infection. Knockdown of UBA2 and Ubc9 limited colony formation to only about 1-2 % in HeLa cells and 4-22 % in U2OS compared to the control population (**Figure 1B and S1A**). We further confirmed these findings by testing cell proliferation of Ubc9 depleted cells four days after infection. Ubc9 knockdown decreased proliferation by 24-45% both in HeLa and U2OS cells (**Figure 1C and S1B**).

Surprisingly, flow cytometry on day four after virus infection did not reveal any significant differences between mock treated cells and cells treated with UBA2 and Ubc9 knockdown viruses (**Figure 1D and S1C**) in contrast to the G2/M block observed in yeast cells lacking Ubc9 [14]. From this we conclude that the decrease in colony formation after UBA2 and Ubc9 knockdown is neither caused by arresting the cells in a specific phase of the cell cycle nor by an increase in the apoptotic cell pool. These findings are consistent with recently reported results [24]. Using BrdU pulse labeling, we could demonstrate a delay in cell cycle progression in response to inhibiting SUMOylation (**Figure 1E and S1D**).

A quantitative proteomics approach to study global SUMOylation dynamics throughout the cell cycle

Subsequently, we were interested in identifying global SUMOylation dynamics during cell cycle progression using a quantitative proteomics approach. SUMOylation proteomics is challenging since SUMOylation levels of most proteins are low and SUMO proteases can rapidly cleave SUMOs from target proteins [25]. To be able to purify SUMO targets from cells, we generated a HeLa cell line stably expressing Flag-tagged SUMO-2 bearing a Q87R mutation in order to shorten the peptide branch remaining after tryptic digestion to enable SUMO acceptor site mapping [26]. SUMO-2 was chosen for these experiments since SUMO-2/3 are the most abundant SUMO family members [27], displaying cell cycle dynamics [28] and mature SUMO-2 and SUMO-3 are virtually identical. Moreover, these SUMO forms are able to form SUMO chains [29, 30] that play an important role in SUMOylation dynamics [31]. Co-expression of GFP, linked to the Flag-SUMO-2 cDNA via an IRES, allowed sorting by flow cytometry of a homogeneous population of low expressing

with control virus four days after infection by adding the cell metabolic activity reagent WST-1 to the growing cells and measuring the absorbance at 450 nm after two hours incubation. The values were normalized to the control and the standard error of the mean was determined from ten values obtained from three independent experiments. ** $p < 0.001$.

D) The graph depicts the percentage of HeLa cells in each cell cycle phase measured by flow cytometry four days after virus infection. Error bars represent the standard deviation from the average obtained from three independent experiments.

E) BrdU pulse chase experiments demonstrate a decelerated passage through the cell cycle for HeLa cells treated with shRNA1 for four days and released from the BrdU pulse for four hours or eight hours. See also Figure S1.

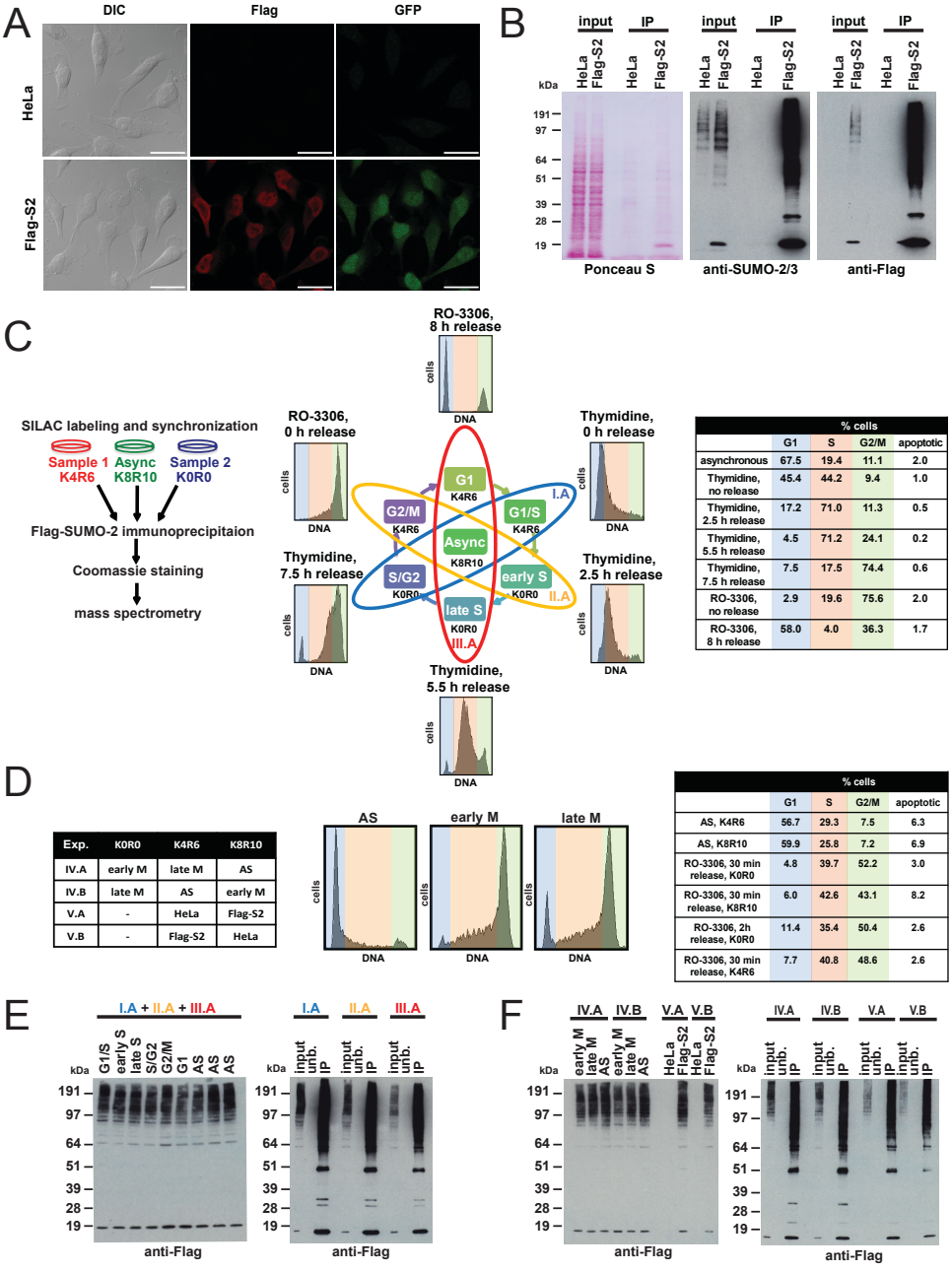

	% cells			
	G1	S	G2/M	apoptotic
asynchronous	67.5	19.4	11.1	2.0
Thymidine, no release	45.4	44.2	9.4	1.0
Thymidine, 2.5 h release	17.2	71.0	11.3	0.5
Thymidine, 5.5 h release	4.5	71.2	24.1	0.2
Thymidine, 7.5 h release	7.5	17.5	74.4	0.6
RO-3306, no release	2.9	19.6	75.6	2.0
RO-3306, 8 h release	58.0	4.0	36.3	1.7

Exp.	K0R0	K4R6	K8R10
IV.A	early M	late M	AS
IV.B	late M	AS	early M
V.A	-	HeLa	Flag-S2
V.B	-	Flag-S2	HeLa

	% cells			
	G1	S	G2/M	apoptotic
AS, K4R6	56.7	29.3	7.5	6.3
AS, K8R10	59.9	25.8	7.2	6.9
RO-3306, 30 min release, K0R0	4.8	39.7	52.2	3.0
RO-3306, 30 min release, K8R10	6.0	42.6	43.1	8.2
RO-3306, 2h release, K0R0	11.4	35.4	50.4	2.6
RO-3306, 30 min release, K4R6	7.7	40.8	48.6	2.6

Figure 2. Global SUMO-2 conjugate dynamics during cell cycle progression

A) HeLa cells were infected with a lentivirus encoding Flag-tagged SUMO-2-Q87R_IRES_GFP, and low expressing cells were sorted by flow cytometry. Flag-SUMO-2 was predominantly located in the nucleus. Scale bars are 25 µm.

B) Expression levels of total SUMO-2/3 and Flag-SUMO-2 conjugates in HeLa cells and Flag-SUMO-2 (Flag-S2) expressing stable cells were compared by immunoblotting. Flag-SUMO-2 conjugates were efficiently purified by IP.

cells to avoid overexpression artifacts.

Analysis of the cells by confocal microscopy revealed that Flag-SUMO-2 was predominantly located in the nucleus as expected (**Figure 2A**). Immunoblotting analysis confirmed the relatively low expression of Flag-SUMO-2 compared to endogenous SUMO-2/3 levels in HeLa cells and the efficient enrichment of SUMO-2 conjugates by immunoprecipitation (IP) (**Figure 2B**).

For quantitative proteomic analysis, three different populations of HeLa cells expressing Flag-SUMO-2 were SILAC labeled with three distinct sets of isotopic variants of lysine and arginine. Cells were blocked with thymidine or the CDK1 inhibitor RO-3306 and either directly lysed or released from the blockage for different amounts of time as indicated in Figure 2C. Flow cytometry analysis confirmed the enrichment of synchronized cell populations at the respective cell cycle stages (**Figure 2C**). Cells released from the RO-3306 block for 8 hours were an exception due to the prolonged presence of G2/M arrested cells. Thus, G1 effects identified in this sample might be underestimated. For subsequent Flag-IP, lysates of synchronized cells were mixed with lysates obtained from asynchronous cells labeled with heavy amino acids as indicated in Figure 2C, resulting in three independent experiments (I.A, II.A and III.A). In addition, we obtained two different M phase-enriched samples (**Figure 2D, 2F and S2B**). Results obtained via flow cytometry confirmed enrichment of arrested cells in the respective cell cycle stage (**Figure 2D**). Asynchronous cells were heavy labeled and mixed with the mitotic samples, resulting in experiment IV.A.

To determine the amount of background binders obtained in this screen, we compared medium labeled asynchronous HeLa cells as a parental control to asynchronous heavy labeled HeLa cells expressing Flag-SUMO-2 (**Figure 2D, 2F and S2B, experiment V.A**). In addition, we performed a complete label-swap control for

C) Strategy to identify SUMO-2 conjugates at different cell cycle stages using a quantitative proteomic approach. HeLa cells stably expressing Flag-SUMO-2 were SILAC-labeled with three different isotopic variants of lysine and arginine and treated as indicated to enrich cells in different phases of the cell cycle. For the Flag-IP, equal amounts of a light labeled and a medium labeled synchronized lysate were mixed with a heavy labeled asynchronous sample resulting in three samples (I.A, II.A and III.A) comprising six different cell cycle stages. Cell cycle synchronization was confirmed by propidium iodide staining and flow cytometry and the percentage of cells in each cell cycle phase is depicted in the table.

D) The left table depicts the combination of samples mixed for experiments IV and V: HeLa cells expressing Flag-SUMO-2 were SILAC-labeled and synchronized with RO-3306 in G2/M. Cells were released from the block for 30 minutes (early M-phase) and 2 hours (late M-phase), respectively. In addition, asynchronous HeLa cells and HeLa cells expressing Flag-SUMO-2 were SILAC-labeled and mixed as indicated in the table to obtain a parental control sample with the according label swap for mass spectrometric analysis. Synchronization of cells was confirmed via flow cytometry. The right table shows the percentage of apoptotic cells and of cells in G1, S and G2/M phase, respectively.

E and F) Total cell lysates of the different synchronized cell pools and purification of Flag-SUMO-2 conjugates by IP were analyzed by immunoblotting using anti-Flag antibody. This was done for experiment I.A, II.A, III.A (E) and experiment IV.A, IV.B, V.A and V.B. (F). See also Figure S2.

A

Results overview	
Raw files	132
Proteins	5180
Peptides	69921
SUMO proteins	593
SUMOylated peptides	356
SUMOylated peptides; unique	203

B

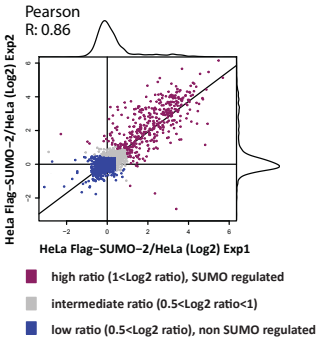

C

Up-and downregulated protein per condition		
	Upregulated	Downregulated
Thymidine, no release	44	7
Thymidine, 2.5h release	14	11
Thymidine, 5.5h release	51	16
Thymidine, 7.5h release	42	16
RO-3306, no release	37	5
RO-3306, 0.5h release	108	44
RO-3306, 2h release	130	26
RO-3306, 8h release	77	11

D

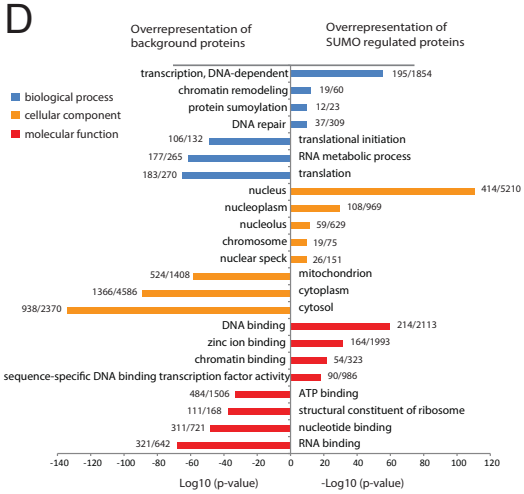

E

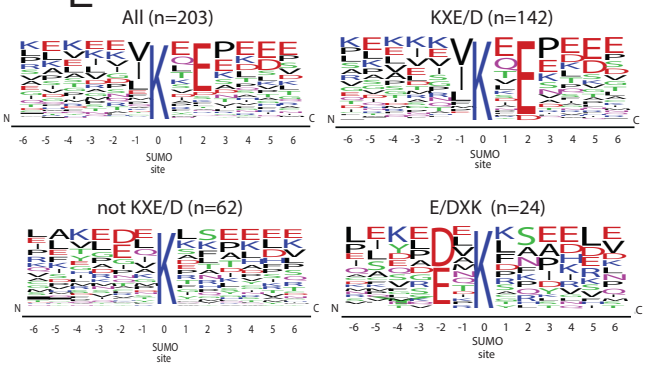

F

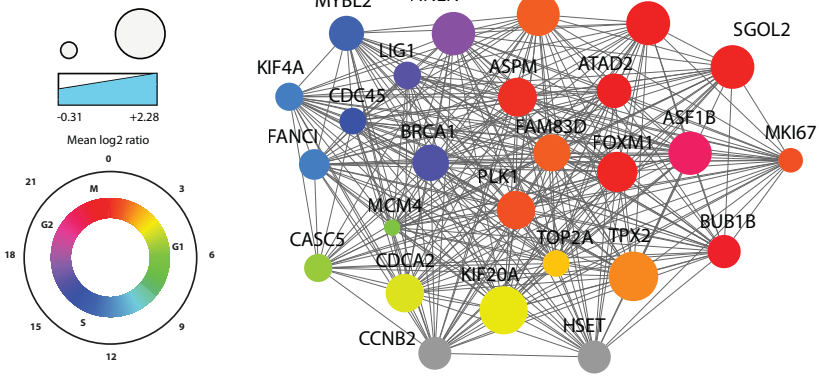

Figure 3. Global SUMOylation dynamics throughout the cell cycle; bioinformatics results
A) Overview of the proteomic experiments. Out of the 5180 proteins identified, 593 proteins were considered as SUMO targets based on SILAC filtering. A total of 356 peptides were identified carrying the QQTGG and/or pyroQQTGG modification, representing 203 unique SUMO-2 acceptor lysines.

all samples (**Figure 2F and S2, experiment I.B-V.B**), which corrects for experimental errors and false positive hits due to light labeled contaminants.

Flag-IP was performed for all ten experiments described and immunoblotting analysis was performed to determine total levels of Flag-SUMO-2 in each input fraction and to confirm highly efficient enrichment for SUMO-2 conjugates by IP (**Figure 2E, 2F, S2D and S2E**). Final eluted fractions of the Flag-IPs were separated by SDS-PAGE, stained with Coomassie, cut in ten gel slices and in-gel digested with trypsin. The Coomassie stained gel of Experiment I.B is shown as an example in Figure S2F. A total of 69,921 unique peptide variants covering 5180 proteins were identified by mass spectrometry at FDR<0.01 and their corresponding SILAC triplets were automatically quantified (**Figure 3A, Table S1**).

To deem a protein SUMOylated, we required a SILAC ratio of at least two between the FLAG-SUMO-2 HeLa cells and the parental control (**Figure 3B, Table S2**). Given the relatively low percentage of cells in G2/M in these control experiments we wanted to avoid excluding SUMO-2 target proteins that peak specifically in G2/M, therefore proteins with a SILAC ratio of at least two in G2/M enriched samples were also included in Table S2. A total of 249 proteins were significantly SUMO-2 up- or downregulated over the cell cycle, as well as 159 with a log2 dynamic range larger than 1.0 (**Figure 3C, Figure S3A**).

SUMOylation dynamics for a subset of the identified SUMO-2 target proteins might be explained by similar dynamics of non-modified forms of these proteins. Therefore, we have analyzed the dynamics of proteins at the total protein

B) SILAC ratio reproducibility plot. Pearson correlation was calculated between both sets of experiments to determine the experimental reproducibility between biological replicates. The Flag-SUMO-2 HeLa cell line was compared to the parental HeLa cell line to determine which proteins were bona-fide SUMO targets. SUMO target proteins with a log2 ratio>1 are indicated in purple, intermediate ratios between 0.5-1 are indicated in grey, whereas non-SUMOylated proteins with log2 ratio <0.5 are colored in dark blue.
C) Overview of upregulated and downregulated SUMOylated proteins in each cell cycle condition. Proteins were filtered for presence in both label-swapped experiments and an average log2 ratio of >0.5 for upregulated targets and <-0.5 for downregulated targets.
D) Gene Ontology (GO) enrichment analysis of SUMO modified proteins versus non–SUMOylated proteins. The bar plot shows the most significantly over-represented GO terms for biological process, cellular component and molecular function for SUMO regulated proteins (Log2 ratio>1) and for non-SUMOylated proteins (Log2 ratio <0.5).
E) SUMO-2 acceptor lysine motif analysis. Weblogo visualization of the amino acid frequencies at each position +/- 6 amino acids from the SUMO-2 acceptor site lysine residues. The size and sorting order of each amino acid indicates its specific frequency at each position and they are colored according to their chemical properties.
F) Functional protein interaction network analysis based on the STRING database. The most significantly interconnected cluster within the total SUMO network visualized by Cytoscape. The cluster is found using the MCODE plug-in and has a MCODE score of 24.4. The functional interactions between proteins are displayed as edges between the proteins (nodes). The cluster has 26 proteins with a total of 305 interactions. The nodes are colored by their estimated cell-cycle peak-time according to the indicated color-scheme and their node size by their highest SILAC log2 ratio. See also Figure S3.

level. We have obtained quantitative information at the total protein level for 361 of the SUMO-2 target proteins, including 27 with a log2 dynamic range larger than 1.0 at the total protein level (**Table S2**).

Gene ontology (GO) enrichment analysis of the SUMO-2 target proteins compared to a background of non-SUMOylated proteins from our dataset revealed a strong overrepresentation of nuclear proteins among the SUMO-2 targets. In particular SUMO modified proteins were highly enriched for sequence-specific DNA transcription factors (**Figure 3D**). Our dataset also contains 356 SUMO-2 modified peptides (**Table S3**) covering 203 unique SUMO acceptor sites (**Table S4**). Sequence motif analysis of the identified sites revealed a strong bias for the SUMO consensus motif **Ψ**KxE (142 sites, **Figure 3E**). We also found 24 sites situated in the previously described inverted SUMO consensus motif [26].

Functional protein interaction network analysis of the SUMO-2 regulated proteins based on the STRING database revealed a highly interconnected protein network (**Figure S3B**). The most significantly connected sub-clusters were identified using the MCODE plug-in for Cytoscape. The most significant cluster with an MCODE score of 24.4 contains 26 SUMO-2 regulated proteins that are color-coded according to their cell cycle peak-time (**Figure 3F**). SUMOylation of the different members of this network is predominantly peaking at that part of the cell cycle where they are functionally most active. For example, FANCI SUMOylation is peaking in S-phase where FANCI is involved in interstrand DNA crosslink repair during replication. ASPM, Aurora-A and –B, PLK1, BUB1B and FoxM1 are peaking in M-phase where they play roles in chromosome condensation and alignment, mitotic spindle formation, and segregation. Two additional functional protein clusters were highlighted by the MCODE analysis (**Figure S3C and S3D**). We demonstrate SUMOylation dynamics throughout the cell cycle by immunoblotting for eleven of the identified SUMO targets (**Figure 4**).

FoxM1 is extensively SUMOylated

The Forkhead box transcription factor M1 (FoxM1) is essential for proper cell cycle progression by regulating a cluster of genes needed for the execution of mitosis [32]. FoxM1 is essential for genome stability since FoxM1 deficiency resulted in aneuploidy. A related phenotype was also observed in a SUMOylation-deficient mouse model, however little is known about relevant SUMO target proteins [17]. We selected FoxM1 for follow-up experiments to study the regulation of this important transcription factor by SUMOylation.

Interestingly, we found an increase in FoxM1 SUMOylation during M-phase in our proteomics project (**Table S2**). Immunoblotting analysis of Flag-SUMO-2 purified fractions showed that SUMOylation of FoxM1 strongly increased mainly in cells blocked at the G2/M border (**Figure 5A**). In asynchronous cells and eight hours after a release from the block, when most cells are in G1 phase (Figure 2C) we observed considerably lower FoxM1 SUMOylation levels. Increases in SUMOylation

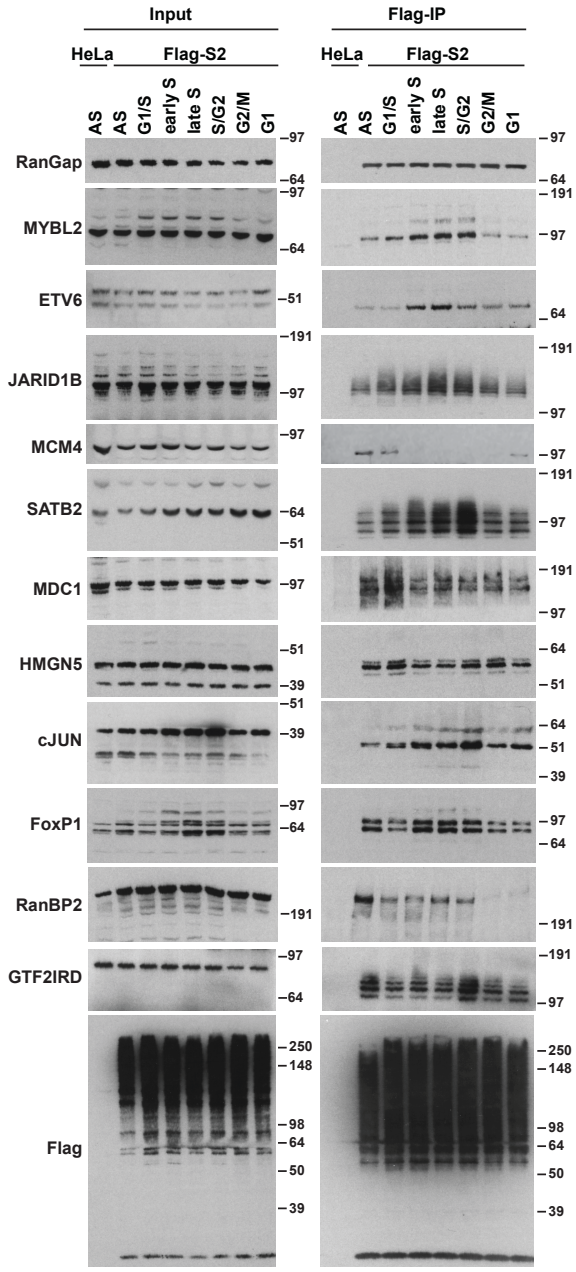

Figure 4. Confirmation of SUMO target proteins by immunoblotting.
HeLa cells stably expressing Flag-tagged SUMO-2 were synchronized at different stages of the cell cycle as described and Flag-SUMO-2 conjugates were purified via IP. Input samples and Flag-SUMO-2 purified fractions were analyzed by immunoblotting with antibodies as indicated. SUMOylation dynamics throughout the cell cycle was demonstrated for eleven different SUMO targets identified in the mass spectrometry screen and RanGAP1 was used as a control. Equal levels of SUMO conjugates in all samples were verified via immunoblotting using anti-Flag antibody. See also Figure S4.

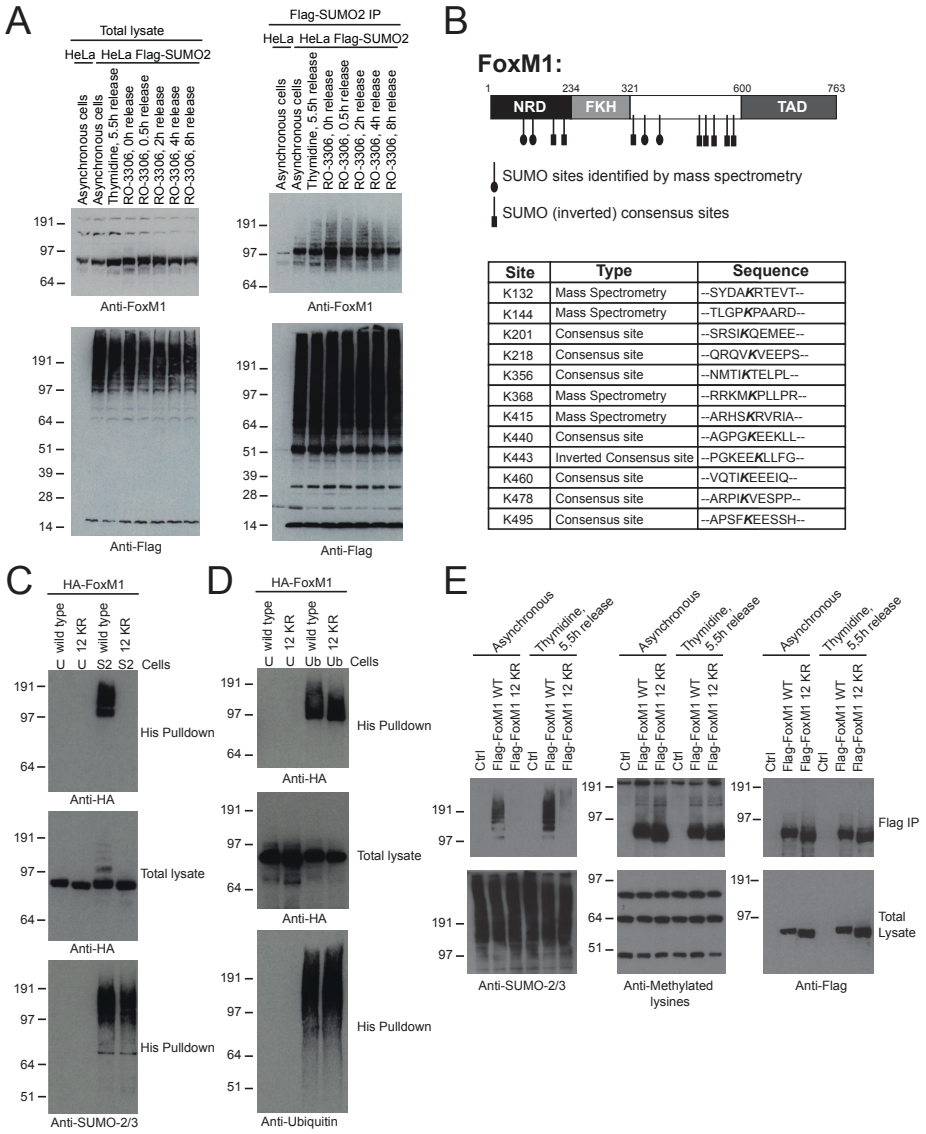

Site	Type	Sequence
K132	Mass Spectrometry	--SYDA***K***RTEVT--
K144	Mass Spectrometry	--TLGP***K***PAARD--
K201	Consensus site	--SRSI***K***QEMEE--
K218	Consensus site	--QRQV***K***VEEPS--
K356	Consensus site	--NMTI***K***TELPL--
K368	Mass Spectrometry	--RRKM***K***PLLPR--
K415	Mass Spectrometry	--ARHS***K***RVRIA--
K440	Consensus site	--AGPG***K***EEKLL--
K443	Inverted Consensus site	--PGKEE***K***LLFG--
K460	Consensus site	--VQTI***K***EEEIQ--
K478	Consensus site	--ARPI***K***VESPP--
K495	Consensus site	--APSF***K***EESSH--

Figure 5. FoxM1 is extensively regulated via SUMOylation

A) HeLa cells stably expressing Flag-SUMO-2 were synchronized with thymidine or RO-3306 and released for different time-points as depicted. Total lysates (left panel) or Flag-SUMO-2 enriched fractions (right panel) were separated by SDS-PAGE, transferred to a membrane, and probed using antibodies to detect FoxM1 or Flag. Asynchronous HeLa cells were used as a negative control for the Flag-SUMO-2 enrichment.

B) Cartoon depicting Forkhead box protein M1 (FoxM1). FoxM1 is composed of 763 amino acids and harbors an N-terminal repressor domain (NRD), a Forkhead winged helix domain (FKH) and a C-terminal transactivation domain (TAD). FoxM1 contains 8 SUMOylation consensus sites and 4 additional SUMOylation sites identified by mass spectrometry.

C) U2OS cells stably expressing His-SUMO-2 (S2) and control U2OS (U) cells were transfected with an expression construct encoding either HA-FoxM1 wild type or HA-FoxM1 lacking the SUMOylation sites (12KR). Cells were lysed 48 hours after transfection in 6 M Guanidine-HCL, and

of FoxM1 can at least partly be explained by increases in total levels of FoxM1 upon synchronization. SUMOylation of FoxM1 was confirmed at the endogenous level (**Figure S5A**).

To study the functional relevance of FoxM1 SUMO modification, we have mapped the SUMO acceptor sites of this protein. FoxM1 has an N-terminal repressor domain (NRD), a Forkhead winged helix DNA binding domain (FKH) and a C-terminal transactivation domain (TAD) (**Figure 5B**). The protein contains seven lysines that are situated in the SUMOylation consensus motif ΨKxE (lysines 201, 218, 356, 440, 460, 478 and 495) and one lysine that is situated in the inverted SUMOylation consensus motif E/DxKΨ (lysine 443). Four additional SUMO acceptor sites that do not represent the classical consensus site were identified by mass-spectrometry analyses of SUMOylated recombinant FoxM1 proteins (**Figure S5B**).

To analyze the SUMOylation of FoxM1, a mutant was generated where these twelve lysines were mutated to arginines (12KR). Wild type and 12KR FoxM1 constructs were expressed in U2OS cells or in U2OS cells stably expressing a His tagged SUMO-2 construct. Analysis of the SUMO enriched fraction confirmed that SUMOylation of FoxM1 was abolished by these mutations (**Figure 5C**). Since FoxM1 is also regulated by ubiquitylation [33], we demonstrated that ubiquitylation of the 12KR mutant is similar to wild-type FoxM1 (**Figure 5D**).

Enrichment of Flag-FoxM1 wild type and Flag-FoxM1 12KR from U2OS cells showed the modification of FoxM1 wild type by endogenous SUMO-2/3 and the increase in SUMOylation of FoxM1 in thymidine released cells (**Figure 5E**). We did not observe modification of the FoxM1 12KR mutant by endogenous SUMO-2/3, further validating our SUMOylation deficient mutant. This experiment was used to confirm that in addition to ubiquitylation, also methylation of FoxM1 is not affected by mutating these twelve lysines, by analyzing Flag-FoxM1 wild type and Flag-FoxM1 12KR enriched fractions by immunoblotting with an antibody directed against methylated-lysine. Nevertheless, some competition between the different PTMs could be observed (**Table S5**).

His-SUMO-2 conjugates were purified by IMAC. Total lysates and purified fractions (His pulldown) were separated by SDS-PAGE, transferred to a membrane, and probed using an antibody to detect HA. Total SUMO-2/3 levels in the purified fractions were detected with a SUMO-2/3 antibody.
D) The experiment described in (C) was repeated in U2OS cells stably expressing His-Ubiquitin (Ub) and control U2OS (U) cells. Ubiquitination of HA-FoxM1 was detected using an antibody directed against the HA-tag. Total ubiquitin levels in the purified fractions were detected by probing immunoblots with an antibody directed against ubiquitin.
E) U2OS cells were transfected with an empty vector (Ctrl), Flag-FoxM1 wild type (WT) or Flag-FoxM1 12KR. Asynchronous cells or cells released for 5.5 hours from a thymidine block were used for Flag-FoxM1 enrichment by Flag-IP. Total lysates (lower panels) and Flag-FoxM1 enriched fractions (upper panels) were separated by SDS-PAGE, transferred to a membrane, and probed using antibodies to detect SUMO-2/3, methylated lysines or Flag. See also Figure S5.

SUMOylation positively regulates FoxM1 transcriptional activity

To study the effect of SUMOylation on the function of FoxM1, we have compared the transcriptional activities of wild-type and SUMOylation-deficient (12KR) FoxM1. In our first approach we used two different luciferase constructs, one containing six FoxM1 DNA binding sites (6x FoxM1 DB-luciferase) and one containing the promoter region of the known FoxM1 target gene *CENP-F* [32]. We found that SUMOylation-deficient FoxM1 was less active compared to wild-type FoxM1, indicating that SUMOylation enhances FoxM1 transcriptional activity (**Figure 6A and 6B**). This observation was further supported by quantitative PCRs (qPCRs) on FoxM1 target genes. Relative mRNA expression levels for *Aurora kinase B*, *Cyclin-B1*, *CENP-F* and *SAP30* were lower in cells stably expressing Flag-FoxM1 12KR compared to cells stably expressing Flag-FoxM1 wild type at similar levels (**Figure 6C and 6D**).

To analyze whether loss of SUMOylation on all twelve lysines of FoxM1 was needed for the reduced activity, we made domain specific FoxM1 SUMOylation mutants in the NRD domain (4KR) or in the undefined domain between the Forkhead and the TAD of FoxM1 (8KR). A small reduction in SUMOylation levels for both mutants indicated modification of both FoxM1 domains (**Figure S6A and S6B**). Consistently, a decreased FoxM1 activity was only observed in the 12KR mutant (**Figure S6C and S6D**). We conclude that FoxM1 is extensively SUMOylated, to increase its transcriptional activity.

Cells expressing SUMOylation-deficient FoxM1 are prone to develop polyploidy

Depletion of FoxM1 expression causes chromosome misalignment and malfunction of cytokinesis, giving rise to the accumulation of tetraploid and polyploid cells [32]. To test whether SUMOylation of FoxM1 is functionally relevant, we set up knockdown and complementation experiments. The stable cell lines described in figure 6C and 6D were used for these assays. Silent mutations were introduced in the Flag-FoxM1 constructs to make them resistant to two independent FoxM1 shRNAs. Cells were infected with a non-targeting control shRNA or with one of the two FoxM1 shRNAs and analyzed three days after infection. Western blot analysis confirmed the efficient knockdown of endogenous FoxM1 in U2OS cells and stable expression of wild-type and SUMOylation-deficient Flag-FoxM1 (**Figure 7A**). Microscopy confirmed that both wild type and SUMOylation-deficient FoxM1 were localized in the nucleus (**Figure S7A**). A similar experiment was performed using GFP tagged FoxM1 to confirm that only endogenous FoxM1 was depleted in the stable cell lines without affecting exogenous FoxM1 (**Figure S7C**). These cells were however not suitable for rescue experiments due to interference of the large GFP tag with FoxM1 protein function.

Cell cycle analysis of the different cell populations confirmed that FoxM1 knockdown resulted in increased populations of tetraploid and polyploid cells. Expression of both FoxM1 wild type and FoxM1 12KR could rescue the knockdown effects on the tetraploid cell population to a similar extent (**Figure S7B**). Also, no

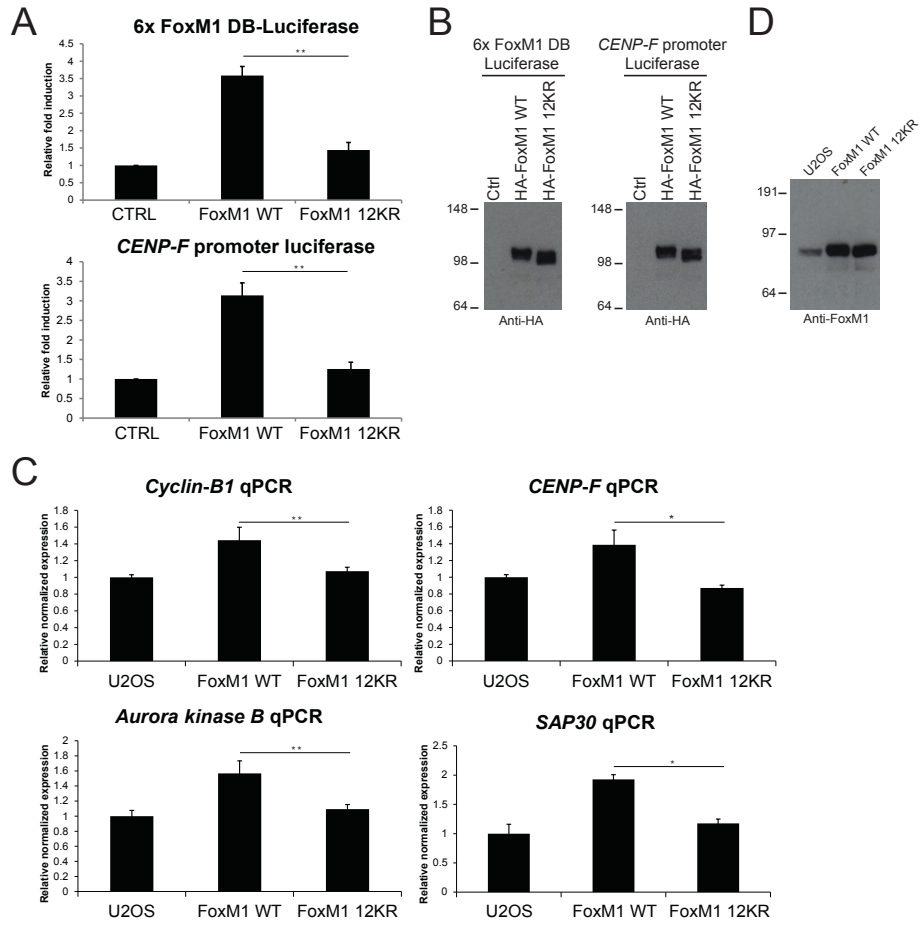

Figure 6. SUMOylation is required for FoxM1 transcriptional activity

A) U2OS cells were (co)transfected with an empty vector, HA-FoxM1 wild type (WT) or HA-FoxM1 12KR, a luciferase reporter containing six FoxM1 DNA binding domains (6x FoxM1 DB-Luciferase, upper panel) or a luciferase reporter containing the *CENP-F* promoter region (lower panel) and a LacZ reporter. Cells were lysed in reporter lysis buffer 48 hours after transfection and luciferase activity and β-galactosidase activity (β-Gal) were measured. Results are representative of six independent experiments and corrected for transfection efficiency using β-Gal activity; the error bars indicate the standard deviation from the average. Results are shown as a relative fold induction compared to cells transfected with the empty vector. ** $p < 0.001$

B) Expression levels of HA-FoxM1 wild-type and HA-FoxM1 12KR proteins in the luciferase experiments were verified by immunoblotting using an antibody directed against the HA-tag.

C) Quantitative PCRs were performed on U2OS cells, U2OS cells stably expressing Flag-FoxM1 wild type or U2OS cells stably expressing Flag-FoxM1 12KR. Primers for *Aurora kinase B*, *Cyclin-B1*,*CENP-F* and *SAP30* were used to quantify specific gene expression. The average expression levels of triplicates were normalized for the expression levels of the housekeeping gene *CAPNS1*. Results for the stable cell lines are shown as relative expression levels compared to U2OS cells (expression level set to 1). ** $p < 0.001$, * $p < 0.05$

D) The expression levels of HA-Flag-FoxM1 wild type and HA-Flag-FoxM1 12KR proteins in the quantitative PCR experiments were verified by immunoblotting using an antibody directed against FoxM1. See also Figure S6.

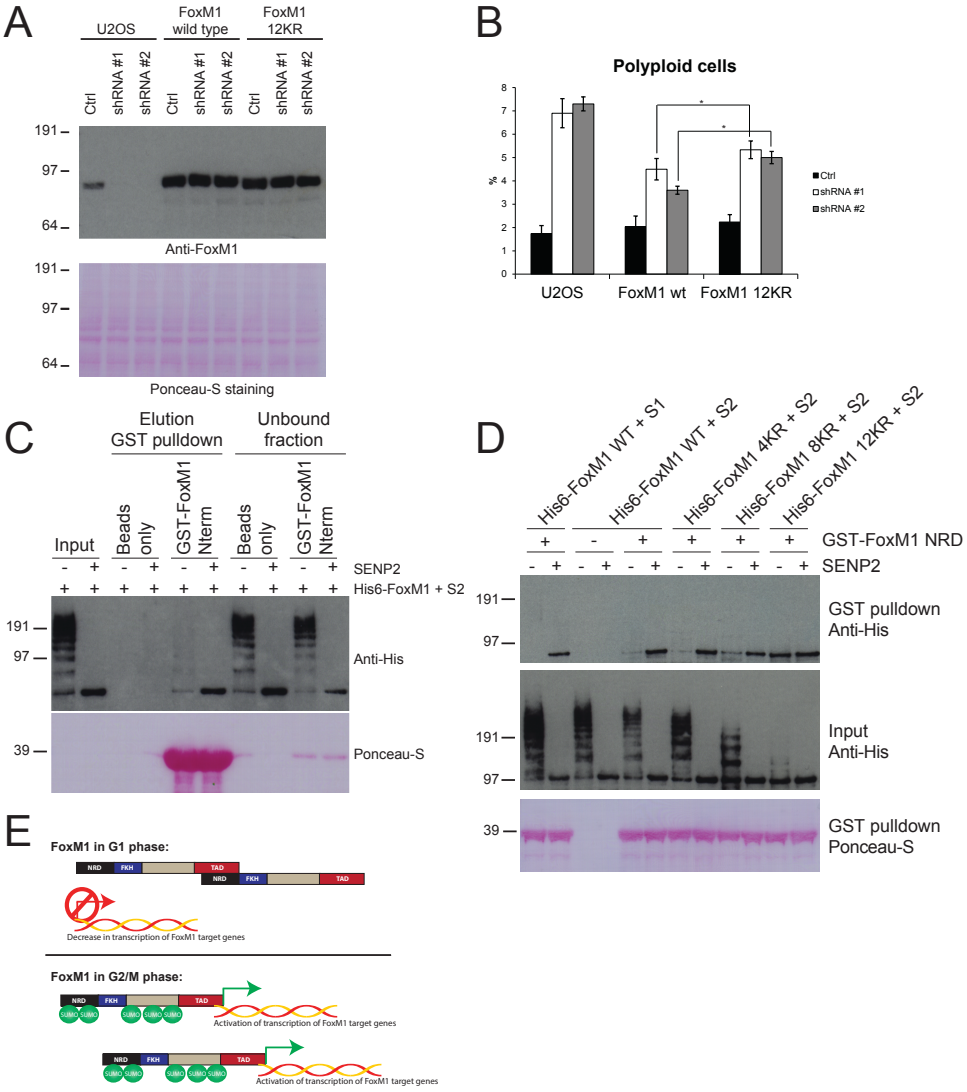

Figure 7. SUMOylation inhibits the negative regulatory domain of FoxM1 and is required to counteract polyploidy

A and B) U2OS cells stably expressing Flag-FoxM1 wild type or Flag-FoxM1 12KR or parental U2OS cells were infected with two individual FoxM1 shRNA lentiviruses (shRNA #1 and shRNA #2) or a non-targeting shRNA (ctrl). Three days after infection cells were harvested for immunoblotting analysis with a FoxM1 antibody (A) and for propidium iodide staining and flow cytometry (B). Average values from three independent experiments are shown in percentages for the polyploid cell population. The error bars indicate the standard deviation from the average. * $p < 0.05$

C) Recombinant His-FoxM1 proteins were SUMOylated *in vitro* and SUMO-2 proteins were removed from His-FoxM1 by incubating the proteins with recombinant SENP2. Glutathione beads only or glutathione beads bound to a GST-FoxM1 N-terminal protein fragment (Nterm) were incubated with SUMOylated His-FoxM1 proteins or His-FoxM1 proteins treated with SENP2. Inputs, elution

obvious differences were found in G1 phase and S phase cell populations when we compared FoxM1 wild type to the SUMOylation-deficient FoxM1 (**Figure S7B**). Interestingly, we observed a significant increase in polyploid cells when comparing cells expressing FoxM1 12KR to FoxM1 wild type cells (**Figure 7B**). Thus, cells deficient for FoxM1 SUMOylation were more sensitive to develop polyploidy.

SUMOylation inhibits the negative regulatory domain of FoxM1

Subsequently, we searched for a mechanistic explanation for the activation of FoxM1 by SUMOylation. In previous studies it was shown that FoxM1 is inhibited in G1 phase via direct interaction between the N-terminal repressor domain and the C-terminal transactivation domain [34, 35]. To study the effects of FoxM1 SUMOylation on this interaction, an *in vitro* interaction assay was performed. A GST tagged N-terminal FoxM1 protein fragment was coupled to glutathione beads and incubated with a mixture of unmodified and SUMOylated His-FoxM1 or unmodified His-FoxM1 proteins only. We observed that only unmodified full-length FoxM1 proteins interacted with the N-terminal part of FoxM1, while SUMOylated FoxM1 did not detectably interact with the protein (**Figure 7C**). By using the domain specific FoxM1 mutants previously described (4KR and 8KR) in this assay, we found that SUMOylation on both the NRD and on the undefined domain of FoxM1 blocks the interaction with the GST tagged NRD protein (**Figure 7D**). His-FoxM1 proteins SUMOylated with SUMO-1 were also unable to interact with the NRD, showing that extensive mono-SUMOylation on the twelve lysines is sufficient to block the interaction since SUMO-1 is impaired for polymerization [30]. Interestingly, even a single modified form of FoxM1 no longer formed dimers. This leads us to propose a model where SUMOylation increases FoxM1 transcriptional activity by inhibiting the interaction between the repressor and activation domain of FoxM1 (**Figure 7E**).

of the GST pulldown and the unbound fraction after the GST pulldown were analyzed by immunoblotting using an antibody directed against the His-tag. The amount of GST-FoxM1 proteins in the elution and the unbound fraction were verified by staining the membrane with Ponceau-S.
D) The experiment described in (C) was repeated using His-FoxM1 wild type (WT) proteins SUMOylated *in vitro* with SUMO-1 and with 3 different His-FoxM1 mutants SUMOylated *in vitro* with SUMO-2; His-FoxM1 4KR, 8KR and 12KR. Inputs and elutions of the GST pulldown were analyzed by immunoblotting and compared to interaction levels of His-FoxM1 WT *in vitro* SUMOylated with SUMO-2.
E) Our data indicate that SUMOylation of FoxM1 during G2 and M phase inhibits the formation of the inactive FoxM1 dimer. This contributes to the increased transcriptional activity of FoxM1 in these phases of the cell cycle. See also Figure S7.

DISCUSSION

We have addressed the role of SUMOylation in cell cycle progression using a proteomics approach to purify and identify hundreds of SUMO target proteins. Co-regulation of these large sets of targets throughout the cell cycle enables orchestration of cell cycle progression via SUMOylation. All aspects of cell cycle progression are influenced by SUMOylation since these target proteins play roles in replication, DNA condensation, chromosome alignment and segregation and cytokinesis. We have also identified 203 SUMO-2 acceptor lysines. Functional analysis of the key mitotic SUMO target protein FoxM1 revealed a role for SUMO-modified FoxM1 in counteracting polyploidy.

Protein group modification

STRING analysis revealed complex interactions between the identified sets of SUMO-2 target proteins (**Figure 3F and S3B**). Half of the SUMOylated proteins depicted in Figure 3F have a known function in mitosis according to their GO biological process term. Interestingly, five of the proteins with SUMOylation peaking in G1/S are established players in the DNA replication pathway. The second most significant MCODE cluster (**Figure S3C**) consists of 11 SUMO-2 regulated proteins that are all involved in mRNA splicing via the spliceosome. The third significant MCODE cluster (**Figure S3D**) consists of 41 SUMOylated proteins of which 16 have transcriptional co-activator activity and seven of them are part of the MLL1 Histone-lysine N-methyltransferase complex.

These results are consistent with previous findings on the role of SUMOylation in yeast in response to DNA damage [36]. In yeast, a set of interacting proteins are SUMOylated and additionally contain SIMs for non-covalent interactions with SUMO. SUMOylation was proposed to act like a molecular glue to enhance group interaction. The networks identified in our screen could similarly be glued together by SUMOylation.

Regulation of FoxM1 via SUMOylation

The Forkhead box (Fox) transcription factor FoxM1 was selected for follow up experiments since this protein links the two major SUMO-regulated biological processes, transcription and the maintenance of genome stability. FoxM1 plays a key role in mitotic progression via transcriptional regulation of a network of genes including *Aurora kinase B*, *CENP-F*, *Cdc25B*, *Cyclin-B1* and *Survivin*. Deregulating the transcription of these genes by depleting FoxM1 expression resulted in a delay in G2 phase, reduced cell proliferation and defects in mitosis. Together these defects in FoxM1 depleted cells resulted in an increased population of cells with a 4*n* DNA content and the formation of aneuploid cells due to missegregation of chromosomes [32, 37]. Previously, Ubc9 deficient cells were shown to have a related phenotype, but relevant SUMO target proteins were still missing [17]. Our data indicate that

FoxM1 is one of the SUMO target proteins relevant for explaining the phenotype of SUMOylation deficient cells.

SUMOylation of transcription factors frequently results in transcriptional inhibition with some exceptions [13, 38, 39] . This is thought to occur via the recruitment of inhibitory complexes. In contrast, SUMOylation is required for activation of FoxM1 (**Figure 6**). Mechanistically, the bulky SUMO modifications prevent the negative regulatory domain from binding to the activation domain, blocking the formation of inactive dimers (**Figure 7**). Consequently, SUMOylated FoxM1 is thought to activate transcription in a monomeric form. Previously, phosphorylation of FoxM1 was proposed to counteract dimer formation [35], but the small size of this modification might be insufficient for full activation of the protein. Phosphorylation and SUMOylation could cooperate to activate FoxM1 via the phosphorylation-dependent SUMOylation motif (PDSM) **Ψ**KxExxS [40], since downstream of K218 in FoxM1, a serine is located at position 223. However, phosphorylation of this serine has so far not been reported [35].

During the revision of our project, another paper was published on the regulation of FoxM1 by SUMOylation [41]. In this paper, the authors claim that the mutation of five SUMOylation consensus motifs in FoxM1 abolished SUMOylation. Using our sensitive method to detect SUMOylation, we found that mutating SUMOylation consensus motifs in FoxM1 was not sufficient to abolish SUMOylation (**Figure S5C**). Whereas Myatt et al. found that SUMOylation inhibited FoxM1, we found that SUMOylation was required for full activity of FoxM1. This discrepancy could be due to the extensive use of a FoxM1-Ubc9 fusion protein by Myatt et al. that was employed to boost SUMOylation and was surprisingly located in the cytoplasm, which might explain its lower transcriptional activity. Furthermore, Myatt et al. enhanced SUMOylation of FoxM1 by transiently overexpressing Ubc9. Using a sensitive method to detect SUMOylation, there was no need for Ubc9 overexpression or the use of a FoxM1-Ubc9 fusion protein in our hands.

FoxM1 plays an important role in cancer and is thought to act as a classical oncogene [42, 43]. Gene expression studies of primary tumors have revealed that FoxM1 is frequently upregulated in solid tumors. High expression levels of FoxM1 have been found in different types of solid tumors including lung, breast, colon, prostate and liver cancer [44, 45]. These hallmarks of elevated FoxM1 expression established the idea that targeting FoxM1 in cancer may have therapeutic advantages [46, 47]. Since SUMOylation of FoxM1 increases FoxM1 transcriptional activity, interfering with FoxM1 SUMOylation might be a potential interesting addition to FoxM1 based cancer therapies. However, currently little is known about the SUMOylation status of FoxM1 in cancer; this is a topic for future studies.

Conclusions and future perspective

Dynamic regulation of a large set of target proteins by SUMOylation plays an important role in cell cycle progression. In this study, we have identified hundreds

of dynamically regulated SUMO-2 target proteins in all stages of the cell cycle using a quantitative proteomics approach and an optimized purification procedure that inactivates SUMO proteases and results in a high yield. The small Flag tag minimally impacts SUMO-2 and is expected not to interfere with SUMOylation dynamics, in contrast to large tags such as GFP that reduce the conjugation rate [48]. Whereas valuable strategies to purify endogenous SUMOs are being developed [49], the yield of these methods is limited compared to the method that we have described here. Optimal yield is required to obtain global insight in SUMOylation dynamics.
Detailed functional analysis of SUMO targets requires the identification of the SUMO acceptor lysines in these proteins to create mutants deficient in SUMOylation. Currently, large-scale site-specific SUMOylation proteomics is still challenging [25, 26, 50]. The set of SUMO acceptor lysines identified in this project is the largest set identified in a single study today, but is still modest and many SUMO-targeted lysines still need to be identified. The site-specific aspect of SUMOylation proteomics still needs further optimizing as it is clearly behind compared to phosphorylation and ubiquitylation. Nevertheless, we believe that the dynamic set of SUMO target proteins identified in this study and the subset of SUMO acceptor sites represents a valuable resource for the scientific community.

EXPERIMENTAL PROCEDURES

Cell lines, Cell culture, SILAC labeling and transfections
HeLa and U2OS cells were cultured in Dulbecco's modified Eagle's medium (Gibco Invitrogen Corporation, Grand Island, NY, USA) supplemented with 10% FCS (Gibco) and 100 U/ml penicillin and 100 μg/ml streptomycin (Gibco). For SILAC analysis, cells were essentially labeled as described before [23]. Transfections were carried out using 2.5 μL polyethylenimine (PEI, 1 mg/ml, Alpha Aesar) per g DNA.

SUMO target protein purification
Cells were lysed in four pellet volumes of lysis buffer (1% SDS, 0.5% NP-40 in PBS including phosphatase - and protease inhibitors). Chloroacetamide was added freshly at 70 mM and samples were sonicated and equalized. An equal volume of dilution buffer (2% Triton X-100, 0.5% sodium deoxycholate, 1% BSA in PBS including phosphatase - and protease inhibitors and freshly added 70 mM chloroacetamide) was added to the lysates and they were centrifuged for 45 minutes at 13.2 krpm at 4ºC. The supernatants were mixed with Flag-M2 beads (Sigma). After 90 minutes incubation, the beads were washed 5 x with wash buffer (50 mM Tris, 150 mM NaCl, 70 mM chloroacetamide, 0.5% NP-40, phosphatase - and protease inhibitors) and bound proteins were eluted.

Mass spectrometry analysis
Purified proteins were size separated by SDS-PAGE, in-gel digested, extracted, desalted, concentrated and analyzed by mass spectrometry using an EASY-nLC system (Proxeon, Odense, Denmark) connected to the LTQ-Orbitrap Velos or to the Q-Exactive (both from Thermo Fisher Scientific, Germany) through a nano-electrospray ion source. Raw mass spectrometry (MS) files were processed with the MaxQuant software suite (version 1.4.0.3, Max Planck Institute of Biochemistry, Department of Proteomics and Signal Transduction, Munich, Germany).

ACKNOWLEDGMENTS

We want to thank Drs. Lars Juhl Jensen and A.G. Jochemsen for advice and Sarah Sparks and Sharareh Sami Abolvardi for technical assistance. We thank Drs. Timmers, De Graaf, Meulmeester and Saitoh for plasmid constructs. This work was supported by the Netherlands Organization for Scientific Research (NWO) (A.C.O.V.). The NNF Center for Protein Research is supported by a generous donation from the Novo Nordisk Foundation. The work was furthermore supported by the Marie Curie Initial Training Networks program of the European Union (290257-UPStream to A.C.O.V. and J.V.O.), and the research career program FSS Sapere Aude (J.V.O.) from the Danish Research Council. None of the authors have a financial interest related to this work.

Reference List

1. Fisher, D., Krasinska, L., Coudreuse, D., and Novak, B. (2012) Phosphorylation network dynamics in the control of cell cycle transitions. *J. Cell Sci.* 125, 4703-4711
2. Kirkin, V., and Dikic, I. (2007) Role of ubiquitin- and Ubl-binding proteins in cell signaling. *Curr. Opin. Cell Biol.* 19, 199-205
3. Wan, J., Subramonian, D., and Zhang, X. D. (2012) SUMOylation in control of accurate chromosome segregation during mitosis. *Curr. Protein Pept. Sci.* 13, 467-481
4. Kirkin, V., and Dikic, I. (2011) Ubiquitin networks in cancer. *Curr. Opin. Genet. Dev.* 21, 21-28
5. Lopez-Otin, C., and Hunter, T. (2010) The regulatory crosstalk between kinases and proteases in cancer. *Nat. Rev. Cancer* 10, 278-292
6. Bettermann, K., Benesch, M., Weis, S., and Haybaeck, J. (2012) SUMOylation in carcinogenesis. *Cancer Lett.* 316, 113-125
7. Zhang, J., Yang, P. L., and Gray, N. S. (2009) Targeting cancer with small molecule kinase inhibitors. *Nat. Rev. Cancer* 9, 28-39
8. Choudhary, C., and Mann, M. (2010) Decoding signalling networks by mass spectrometry-based proteomics. *Nat. Rev. Mol. Cell Biol.* 11, 427-439
9. Olsen, J. V. et al. (2010) Quantitative phosphoproteomics reveals widespread full phosphorylation site occupancy during mitosis. *Sci. Signal.* 3, ra3
10. Gareau, J. R., and Lima, C. D. (2010) The SUMO pathway: emerging mechanisms that shape specificity, conjugation and recognition. *Nat. Rev. Mol. Cell Biol.* 11, 861-871
11. Hay, R. T. (2005) SUMO: a history of modification. *Mol. Cell* 18, 1-12
12. Geiss-Friedlander, R., and Melchior, F. (2007) Concepts in sumoylation: a decade on. *Nat. Rev. Mol. Cell Biol.* 8, 947-956
13. Flotho, A., and Melchior, F. (2013) Sumoylation: a regulatory protein modification in health and disease. *Annu. Rev. Biochem.* 82, 357-385
14. Seufert, W., Futcher, B., and Jentsch, S. (1995) Role of a ubiquitin-conjugating enzyme in degradation of S- and M-phase cyclins. *Nature* 373, 78-81
15. Li, S. J., and Hochstrasser, M. (1999) A new protease required for cell-cycle progression in yeast. *Nature* 398, 246-251
16. Schwartz, D. C., Felberbaum, R., and Hochstrasser, M. (2007) The Ulp2 SUMO protease

is required for cell division following termination of the DNA damage checkpoint. *Mol. Cell Biol.* 27, 6948-6961

17. Nacerddine, K. et al. (2005) The SUMO pathway is essential for nuclear integrity and chromosome segregation in mice. *Dev. Cell* 9, 769-779
18. Ulrich, H. D. (2009) Regulating post-translational modifications of the eukaryotic replication clamp PCNA. *DNA Repair (Amst)* 8, 461-469
19. Armstrong, A. A., Mohideen, F., and Lima, C. D. (2012) Recognition of SUMO-modified PCNA requires tandem receptor motifs in Srs2. *Nature* 483, 59-63
20. Dawlaty, M. M. et al. (2008) Resolution of sister centromeres requires RanBP2-mediated SUMOylation of topoisomerase IIalpha. *Cell* 133, 103-115
21. Mukhopadhyay, D., Arnaoutov, A., and Dasso, M. (2010) The SUMO protease SENP6 is essential for inner kinetochore assembly. *J. Cell Biol.* 188, 681-692
22. Klein, U. R., Haindl, M., Nigg, E. A., and Muller, S. (2009) RanBP2 and SENP3 function in a mitotic SUMO2/3 conjugation-deconjugation cycle on Borealin. *Mol. Biol. Cell* 20, 410-418
23. Mann, M. (2006) Functional and quantitative proteomics using SILAC. *Nat. Rev. Mol. Cell Biol.* 7, 952-958
24. Neyret-Kahn, H. et al. (2013) Sumoylation at chromatin governs coordinated repression of a transcriptional program essential for cell growth and proliferation. *Genome Res.* 23, 1563-1579
25. Vertegaal, A. C. (2011) Uncovering ubiquitin and ubiquitin-like signaling networks. *Chem. Rev.* 111, 7923-7940
26. Matic, I. et al. (2010) Site-specific identification of SUMO-2 targets in cells reveals an inverted SUMOylation motif and a hydrophobic cluster SUMOylation motif. *Mol. Cell* 39, 641-652
27. Saitoh, H., and Hinchey, J. (2000) Functional heterogeneity of small ubiquitin-related protein modifiers SUMO-1 versus SUMO-2/3. *J. Biol. Chem.* 275, 6252-6258
28. Zhang, X. D. et al. (2008) SUMO-2/3 modification and binding regulate the association of CENP-E with kinetochores and progression through mitosis. *Mol. Cell* 29, 729-741
29. Tatham, M. H. et al. (2001) Polymeric chains of SUMO-2 and SUMO-3 are conjugated to protein substrates by SAE1/SAE2 and Ubc9. *J. Biol. Chem.* 276, 35368-35374
30. Matic, I. et al. (2008) In vivo identification of human small ubiquitin-like modifier polymerization sites by high accuracy mass spectrometry and an in vitro to in vivo strategy. *Mol. Cell Proteomics* 7, 132-144
31. Tatham, M. H. et al. (2008) RNF4 is a poly-SUMO-specific E3 ubiquitin ligase required for arsenic-induced PML degradation. *Nat. Cell Biol.* 10, 538-546
32. Laoukili, J. et al. (2005) FoxM1 is required for execution of the mitotic programme and chromosome stability. *Nat. Cell Biol.* 7, 126-136
33. Laoukili, J., Alvarez-Fernandez, M., Stahl, M., and Medema, R. H. (2008) FoxM1 is degraded at mitotic exit in a Cdh1-dependent manner. *Cell Cycle* 7, 2720-2726
34. Park, H. J. et al. (2008) An N-terminal inhibitory domain modulates activity of FoxM1 during cell cycle. *Oncogene* 27, 1696-1704
35. Laoukili, J. et al. (2008) Activation of FoxM1 during G2 requires cyclin A/Cdk-dependent relief of autorepression by the FoxM1 N-terminal domain. *Mol. Cell Biol.* 28, 3076-3087
36. Psakhye, I., and Jentsch, S. (2012) Protein group modification and synergy in the SUMO pathway as exemplified in DNA repair. *Cell* 151, 807-820

37. Wang, I. C. et al. (2005) Forkhead box M1 regulates the transcriptional network of genes essential for mitotic progression and genes encoding the SCF (Skp2-Cks1) ubiquitin ligase. *Mol. Cell Biol.* 25, 10875-10894
38. Ouyang, J., Valin, A., and Gill, G. (2009) Regulation of transcription factor activity by SUMO modification. *Methods Mol. Biol.* 497, 141-152
39. Lyst, M. J., and Stancheva, I. (2007) A role for SUMO modification in transcriptional repression and activation. *Biochem. Soc. Trans.* 35, 1389-1392
40. Hietakangas, V. et al. (2006) PDSM, a motif for phosphorylation-dependent SUMO modification. *Proc. Natl. Acad. Sci. U. S. A* 103, 45-50
41. Myatt, S. S. et al. (2013) SUMOylation inhibits FOXM1 activity and delays mitotic transition. *Oncogene*
42. Zhao, F., and Lam, E. W. (2012) Role of the forkhead transcription factor FOXO-FOXM1 axis in cancer and drug resistance. *Front Med.* 6, 376-380
43. Anders, L. et al. (2011) A systematic screen for CDK4/6 substrates links FOXM1 phosphorylation to senescence suppression in cancer cells. *Cancer Cell* 20, 620-634
44. Koo, C. Y., Muir, K. W., and Lam, E. W. (2012) FOXM1: From cancer initiation to progression and treatment. *Biochim. Biophys. Acta* 1819, 28-37
45. Wierstra, I. (2013) FOXM1 (Forkhead box M1) in tumorigenesis: overexpression in human cancer, implication in tumorigenesis, oncogenic functions, tumor-suppressive properties, and target of anticancer therapy. *Adv. Cancer Res.* 119, 191-419
46. Radhakrishnan, S. K. et al. (2006) Identification of a chemical inhibitor of the oncogenic transcription factor forkhead box M1. *Cancer Res.* 66, 9731-9735
47. Halasi, M., and Gartel, A. L. (2013) Targeting FOXM1 in cancer. *Biochem. Pharmacol.* 85, 644-652
48. Vertegaal, A. C. et al. (2004) A proteomic study of SUMO-2 target proteins. *J. Biol. Chem.* 279, 33791-33798
49. Becker, J. et al. (2013) Detecting endogenous SUMO targets in mammalian cells and tissues. *Nat. Struct. Mol. Biol.* 20, 525-531
50. Hsiao, H. H., Meulmeester, E., Frank, B. T., Melchior, F., and Urlaub, H. (2009) "ChopNSpice," a mass spectrometric approach that allows identification of endogenous small ubiquitin-like modifier-conjugated peptides. *Mol. Cell Proteomics* 8, 2664-2675

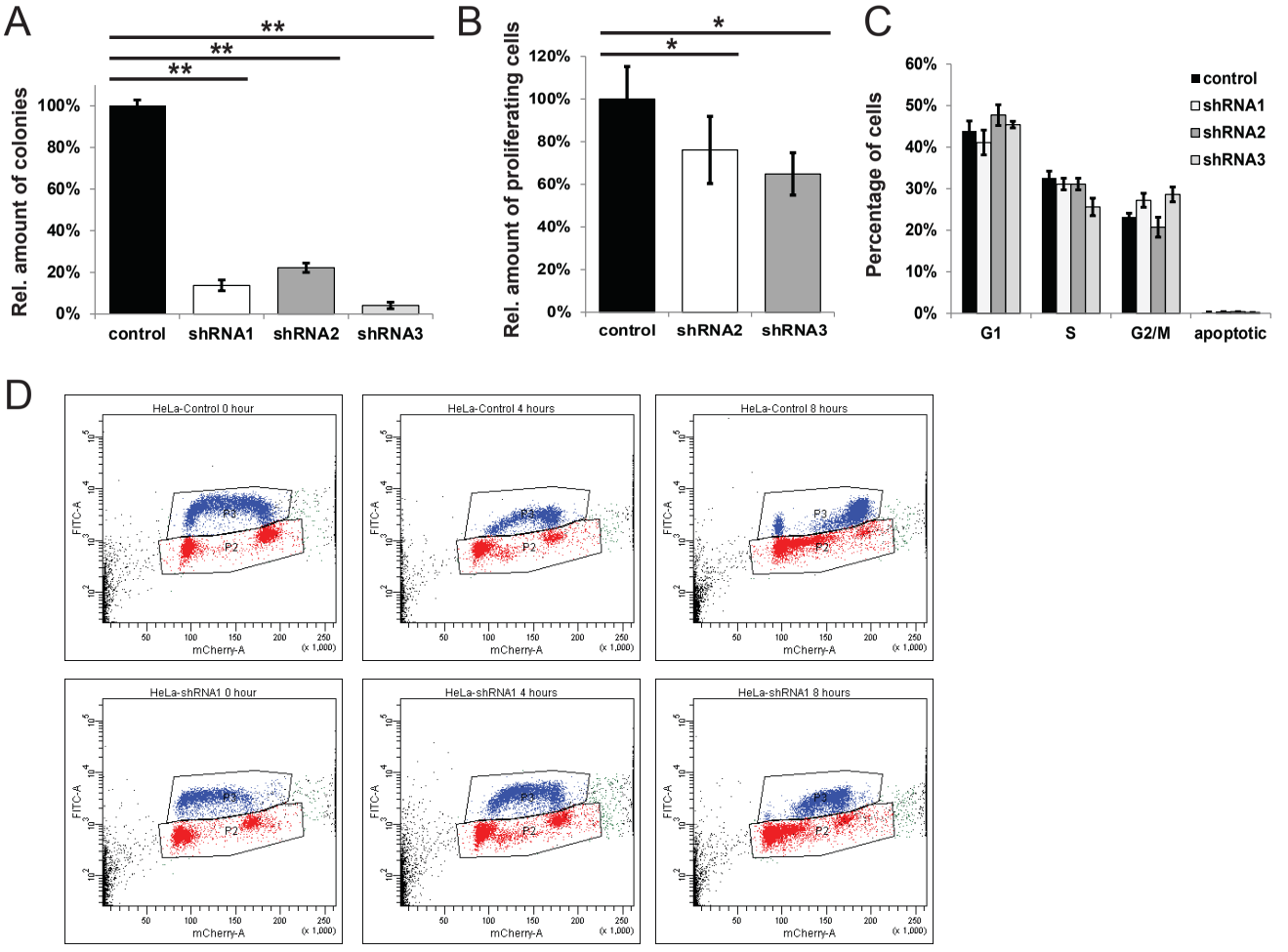
A
Rel. amount of colonies
100%
80%
60%
40%
20%
0%
**
**
**
control
shRNA1
shRNA2
shRNA3
B
Rel. amount of proliferating cells
120%
100%
80%
60%
40%
20%
0%
*
*
control
shRNA2
shRNA3
C
Percentage of cells
60%
50%
40%
30%
20%
10%
0%
control
shRNA1
shRNA2
shRNA3
G1
S
G2/M
apoptotic
D
HeLa-Control 0 hour
HeLa-Control 4 hours
HeLa-Control 8 hours
HeLa-shRNA1 0 hour
HeLa-shRNA1 4 hours
HeLa-shRNA1 8 hours
FITC-A
mCherry-A
(x 1,000)
P1
P2
P3

Figure S1. Cell cycle profile after UBA2 and Ubc9 knockdown.
A) Colony formation of U2OS cells was determined nine days after infection with a control shRNA, shRNA1 (UBA2), shRNA2 or shRNA3 (both Ubc9) by staining with Giemsa solution and counting colonies using the ImageJ Version 1.47v software. The values were normalized to the control. Error bars represent the standard deviation from the average obtained from three independent experiments. ** $p < 0.001$.
B) The proliferation rate of U2OS cells treated with Ubc9 knockdown virus was compared to cells treated with control virus four days after infection by adding the cell proliferation reagent WST-1 to the growing cells and measuring the absorbance at 450 nm after two hours incubation. The values were normalized to the control and the standard error of the mean was determined from ten values obtained from three independent experiments. * $p < 0.05$.
C) Four days after infection with UBA2, Ubc9 and control viruses, U2OS cells were stained with propidium iodide and subjected to flow cytometry analysis. The graph depicts the percentage of cells in each cell cycle phase. Error bars represent the standard deviation from the average obtained from three independent experiments.
D) HeLa cells treated with control shRNA and shRNA1 for four days were pulse-labeled with BrdU and released for four hours or eight hours before staining them with propidium iodide. The graphs depict the amount of DNA (mCherry-A) in BrdU labeled cells (blue) and non-labeled cells (red) at the respective time-points demonstrating a faster passage through the cell cycle for the control compared to cells with a reduced UBA2 expression.

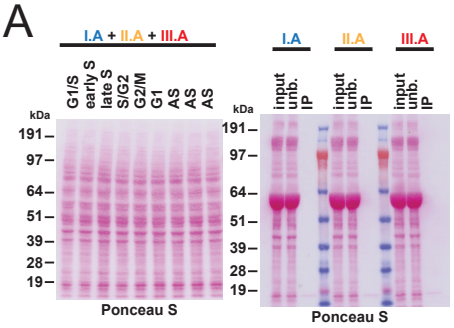

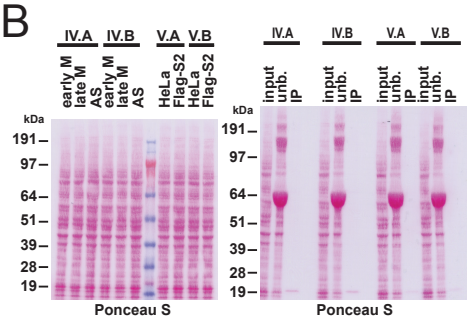

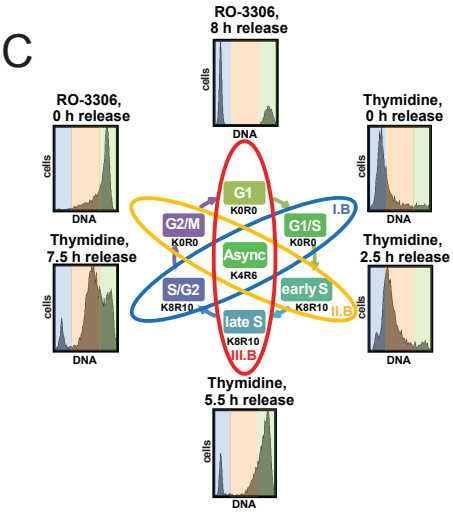

	% cells			
	G1	S	G2/M	apoptotic
async	64.1	16.2	14.6	4.4
Thymidine, no release	47.5	39.5	7.3	4.7
Thymidine, 2.5 h release	16.7	71.4	9.1	2.0
Thymidine, 5.5 h release	7.5	46.6	41.4	1.5
Thymidine, 7.5 h release	13.2	14.4	66.6	2.5
RO-3306, no release	3.1	23.2	68.7	4.5
RO-3306, 8 h release	62.5	3.1	29.9	3.0

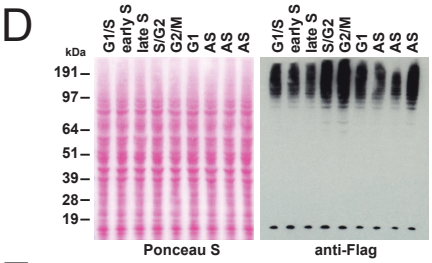

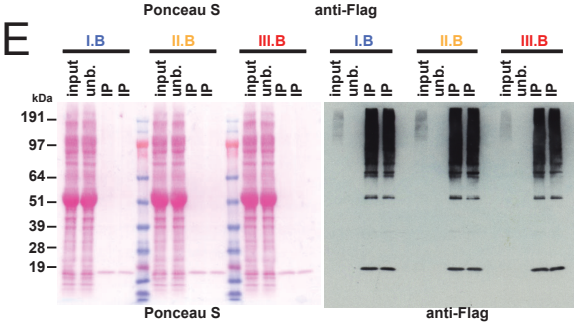

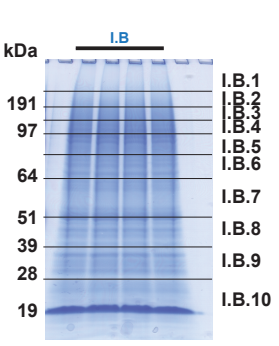

Figure S2. Loading controls and label swap of SILAC-labeled cells synchronized in different cell cycle stages and purification of SUMO conjugates.
A) HeLa cells stably expressing Flag-SUMO-2 were SILAC-labeled with three different isotopic variants of lysine and arginine. Three independent pools of light labeled (K0R0) cells and one pool of medium labeled (K4R6) cells were blocked with thymidine. Two pools of medium labeled cells were blocked with RO-3306. The light labeled cells were released from the thymidine block and lysed at three different time points (2.5 hours, 5.5 hours and 7.5 hours after release). Two pools of medium labeled cells were lysed directly after the thymidine block or the RO-3306 block. The third medium labeled pool was released from the RO-3306 block for eight hours and then lysed. Three pools of asynchronous cells were heavy labeled (K8R10) and served as an internal standard during the subsequent analysis. Total cell lysates of the different synchronized cell pools were size separated by SDS-PAGE and levels were analyzed by Ponceau S staining (left panel). For the Flag-immunoprecipitation, equal amounts of lysates from light-labeled and heavy-labeled synchronized cells were mixed with an equal amount of lysate from medium-labeled asynchronous cells, resulting in three samples (I.B, II.B and III.B) comprising six time points in cell cycle progression. Inputs, unbound fractions and immunoprecipitated samples were analyzed by Ponceau S staining (right panel).
B) HeLa cells expressing Flag-SUMO-2 were SILAC-labeled and synchronized with RO-3306 in G2/M. Cells were released from the block for 30 minutes (early M-phase) and 2 hours (late M-phase), respectively (experiment IV.A and label swap experiment IV.B). In addition, asynchronous HeLa cells and asynchronous HeLa cells expressing Flag-SUMO-2 were SILAC-labeled and mixed to obtain a parental control sample for mass spectrometric analysis (experiment V.A and label swap experiment V.B). Total cell lysates of the different cell pools were size separated by SDS-PAGE and levels were analyzed by Ponceau S staining (left panel). Inputs, unbound fractions and immunoprecipitated samples were analyzed by Ponceau S staining (right panel).
C) Label swap for the experiment described in (A). Cell cycle synchronization was confirmed by flow cytometry. Flow cytometry profiles are shown next to the respective samples and the percentage of cells in each cell cycle phase is depicted in the table.
D) Lysates of the different synchronized cell pools from the experiment described in (C) were size-separated by SDS-PAGE and protein levels were analyzed by Ponceau S staining (left panel), levels of Flag-SUMO-2 conjugates were compared by immunoblotting using an antibody directed against the Flag epitope (right panel).
E) Purification of Flag-SUMO-2 conjugates by immunoprecipitation in the experiment described in (C) was confirmed by immunoblotting for all three experiments. Inputs, unbound fractions and immunoprecipitated samples were size-separated by SDS-PAGE and levels were analyzed by Ponceau S staining (left panel). Levels of Flag-SUMO-2 conjugates were analyzed by immunoblotting using an antibody directed against the Flag epitope (right panel).
F) The Flag-IP samples of all three experiments described in (C) were size separated by SDS-PAGE and stained with Coomassie. Each sample was divided into ten different gel slices according to the molecular weight of the purified proteins. These sections were further cut into small gel fragments, proteins were digested by trypsin, extracted and analyzed by mass spectrometry. The Coomassie stained gel for experiment I.B is shown as an example.

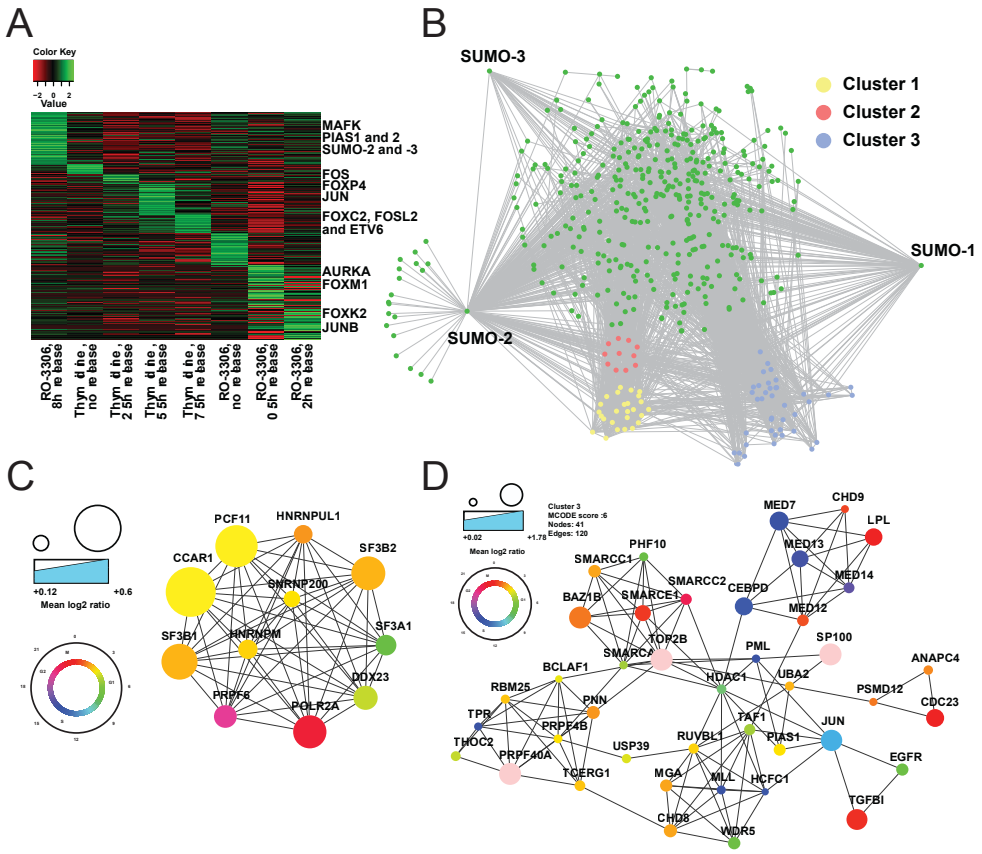

Figure S3. Global SUMOylation dynamics throughout the cell cycle.

A) A standardized heat map of SUMOylated proteins. Red indicates a low SILAC Log2 ratio while green indicates a high SILAC Log2 ratio of the SUMO target proteins at the different time points in the experiment.

B) The total functional SUMO protein network. The STRING network including 474 nodes with 2538 edges was acquired and visualized in Cytoscape. The MCODE plugin for Cytoscape was used to find highly interconnected clusters within the network. The three most interconnected clusters in the total network are highlighted.

C) The second most significantly interconnected cluster within the total SUMO network. The cluster contains 11 proteins with a total of 55 interactions. The nodes are colored by their estimated cell-cycle peak-time according to the indicated color-scheme and their node size by their highest SILAC log2 ratio.

D) The third most significantly interconnected cluster within the total SUMO network. The cluster contains 41 proteins with a total of 120 interactions. The nodes are colored by their estimated cell-cycle peak-time according to the indicated color-scheme and their node size by their highest SILAC log2 ratio.

	% cells			
	G1	S	G2/M	apoptotic
asynchronous	55.8	20.8	23.0	0.4
Thymidine, no release	33.2	58.8	7.1	0.9
Thymidine, 2.5 h release	5.6	83.2	10.9	0.3
Thymidine, 5.5 h release	5.6	70.8	23.2	0.4
Thymidine, 7.5 h release	11.1	28.9	59.6	0.4
RO-3306, no release	1.2	21.5	75.3	2.0
RO-3306, 8 h release	62.2	5.5	29.4	2.9

Figure S4. Flow cytometry analysis of cell cycle synchronization.
HeLa cells stably expressing Flag-SUMO-2 were synchronized in different stages of the cell cycle as previous described. Cell cycle synchronization was confirmed by flow cytometry, the percentage of cells in each cell cycle phase is depicted in the table.

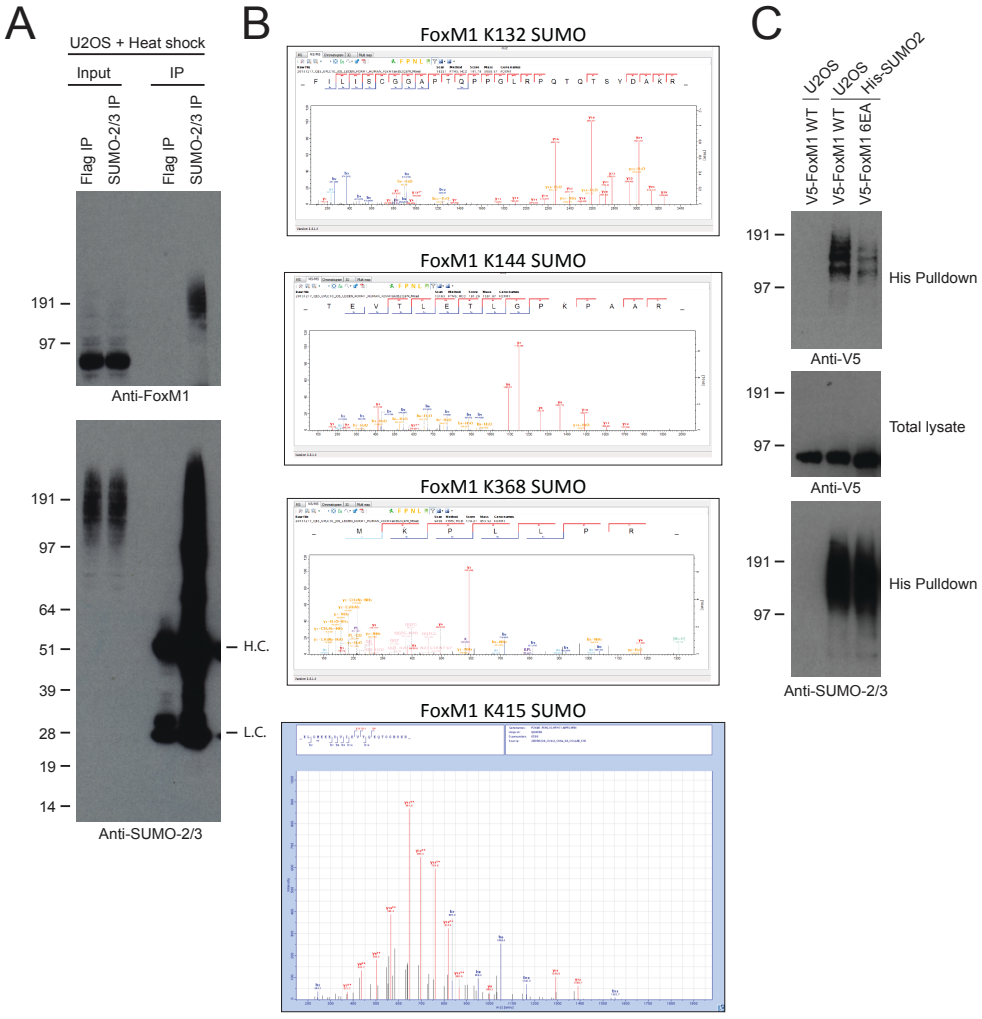
A
U2OS + Heat shock
Input
IP
Flag IP
SUMO-2/3 IP
Flag IP
SUMO-2/3 IP
191
97
Anti-FoxM1
191
97
64
51
39
28
19
14
H.C.
L.C.
Anti-SUMO-2/3
B
FoxM1 K132 SUMO
FoxM1 K144 SUMO
FoxM1 K368 SUMO
FoxM1 K415 SUMO
C
U2OS
U2OS
His-SUMO2
V5-FoxM1 WT
V5-FoxM1 WT
V5-FoxM1 6EA
191
97
His Pulldown
Anti-V5
191
97
Total lysate
Anti-V5
191
97
His Pulldown
Anti-SUMO-2/3

Figure S5. Endogenous FoxM1 SUMOylation and identification of SUMO-2 acceptor sites in FoxM1.

A) U2OS cells were exposed to heat shock at 43°C for 1 hour to destabilize SUMO proteases and subsequently lysed for immunoprecipitation with a mouse monoclonal SUMO-2/3 antibody or a Flag antibody as a control. Input and IP samples were size separated by SDS-PAGE and analyzed by immunoblotting using FoxM1 antibody (upper panel) or SUMO-2/3 antibody (lower panel). Heavy Chains (H.C) and Light Chains (L.C) of the antibodies are indicated.

B) MS/MS spectra for the SUMO acceptor sites in FoxM1. K132, K144 and K368 were found to be SUMO-2 modified in human FoxM1. Additionally K415 was found to be SUMO-1 modified in mouse FoxM1; this lysine is conserved in human FoxM1.

C) U2OS cells stably expressing His-SUMO-2 were transfected with expression constructs encoding mouse V5-FoxM1 WT or V5-FoxM1 6EA (E201A, E218A, E356A, E461A, E479A and E496A). The six consensus sites mutated in this construct are conserved in human FoxM1. U2OS cells were transfected with a V5-FoxM1 WT construct as a control. Cells were lysed 48 hours after transfection in 6 M Guanidine-HCL, and His-SUMO-2 conjugates were purified by immobilized metal ion affinity chromatography. Total lysates and purified fractions (His pulldown) were separated by SDS-PAGE, transferred to a membrane, and probed using an antibody to detect V5. Total SUMO-2/3 levels in the purified fractions were detected with a SUMO-2/3 antibody.

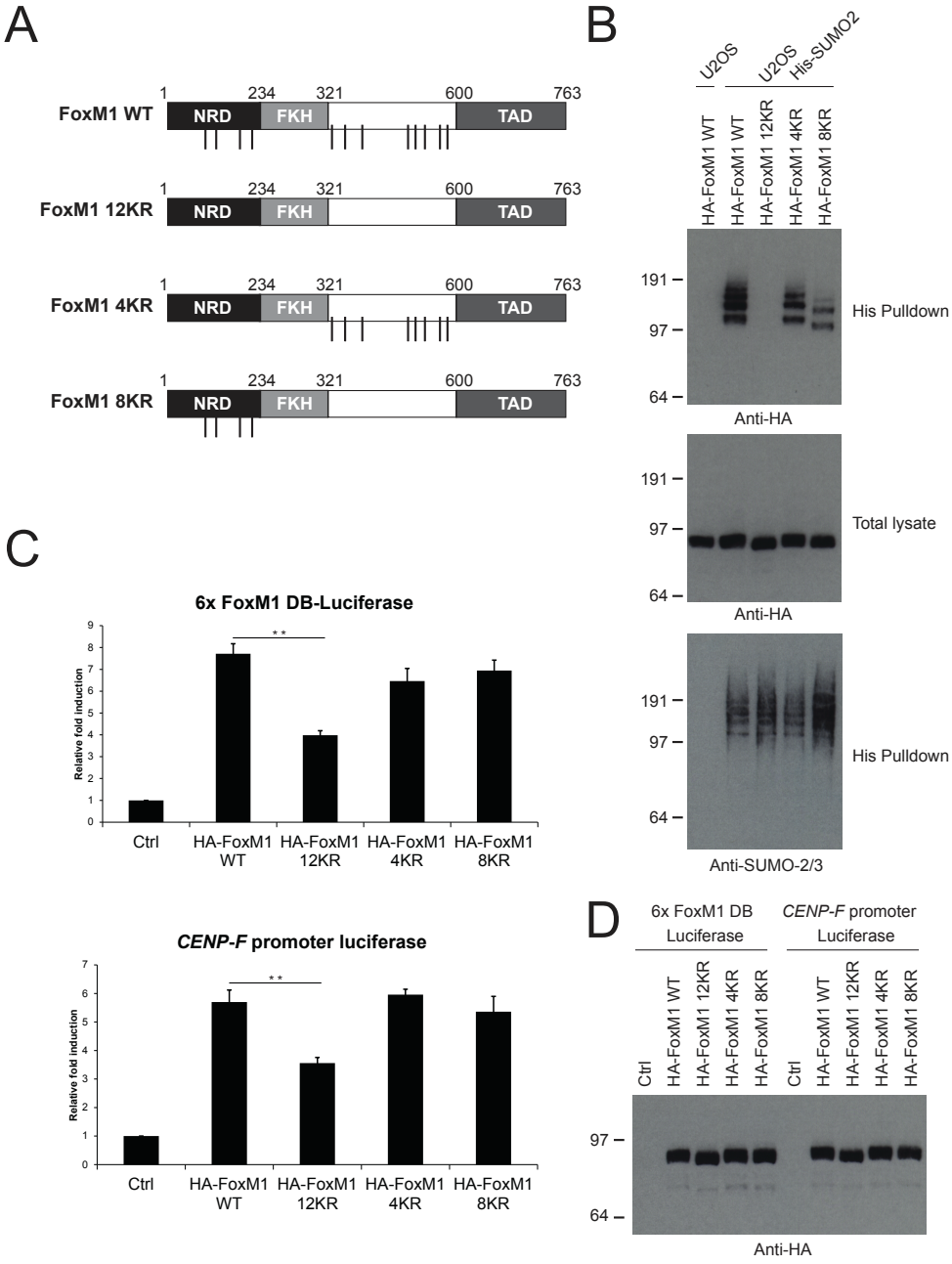
A
FoxM1 WT
FoxM1 12KR
FoxM1 4KR
FoxM1 8KR
1
234
321
600
763
NRD
FKH
TAD
B
U2OS
U2OS
His-SUMO2
HA-FoxM1 WT
HA-FoxM1 WT
HA-FoxM1 12KR
HA-FoxM1 4KR
HA-FoxM1 8KR
191
97
64
His Pulldown
Anti-HA
Total lysate
Anti-HA
His Pulldown
Anti-SUMO-2/3
C
6x FoxM1 DB-Luciferase
Relative fold induction
Ctrl
HA-FoxM1 WT
HA-FoxM1 12KR
HA-FoxM1 4KR
HA-FoxM1 8KR
CENP-F promoter luciferase
D
6x FoxM1 DB Luciferase
CENP-F promoter Luciferase
Ctrl
HA-FoxM1 WT
HA-FoxM1 12KR
HA-FoxM1 4KR
HA-FoxM1 8KR
97
64
Anti-HA

Figure S6. Analysis of domain specific FoxM1 SUMOylation mutants.
A) Different FoxM1 mutants were generated. The four lysines in the N terminal repressor domain (4KR) or the eight lysines in the undefined domain between the Forkhead and the C terminal trans-activation domain (8KR) were mutated to arginines. These mutants were compared to wild-type (WT) FoxM1 and the 12KR mutant of FoxM1.
B) U2OS cells stably expressing His-SUMO-2 were transfected with expression constructs encoding HA-FoxM1 WT, HA-FoxM1 12KR, HA-FoxM1 4KR or HA-FoxM1 8KR. U2OS cells were transfected with HA-FoxM1 WT as a control. Cells were lysed 48 hours after transfection in 6 M Guanidine-HCL, and His-SUMO-2 conjugates were purified by immobilized metal ion affinity chromatography. Total lysates and purified fractions (His pulldown) were separated by SDS-PAGE, transferred to a membrane, and probed using an antibody to detect HA. Total SUMO-2/3 levels in the purified fractions were detected with an antibody directed against SUMO-2/3.
C) U2OS cells were co-transfected with an empty vector, HA-FoxM1 WT, HA-FoxM1 12KR, HA-FoxM1 4KR or HA-FoxM1 8KR and a luciferase reporter containing six FoxM1 DNA binding domains (6x FoxM1 DB-Luciferase, upper panel) or a luciferase reporter containing the *CENP-F* promoter region (lower panel) and a LacZ reporter. Cells were lysed in reporter lysis buffer 48 hours after transfection and luciferase activity and β-gal activity were measured. Results are representative of four independent experiments and corrected for transfection efficiency using β-gal activity; the error bars indicate the standard deviation from the average. Results are shown as a relative fold induction compared to cells transfected with the empty vector. ** $p < 0.001$
D) Expression levels of the different HA-FoxM1 proteins in the luciferase experiments were verified by immunoblotting using an antibody directed against the HA-tag.

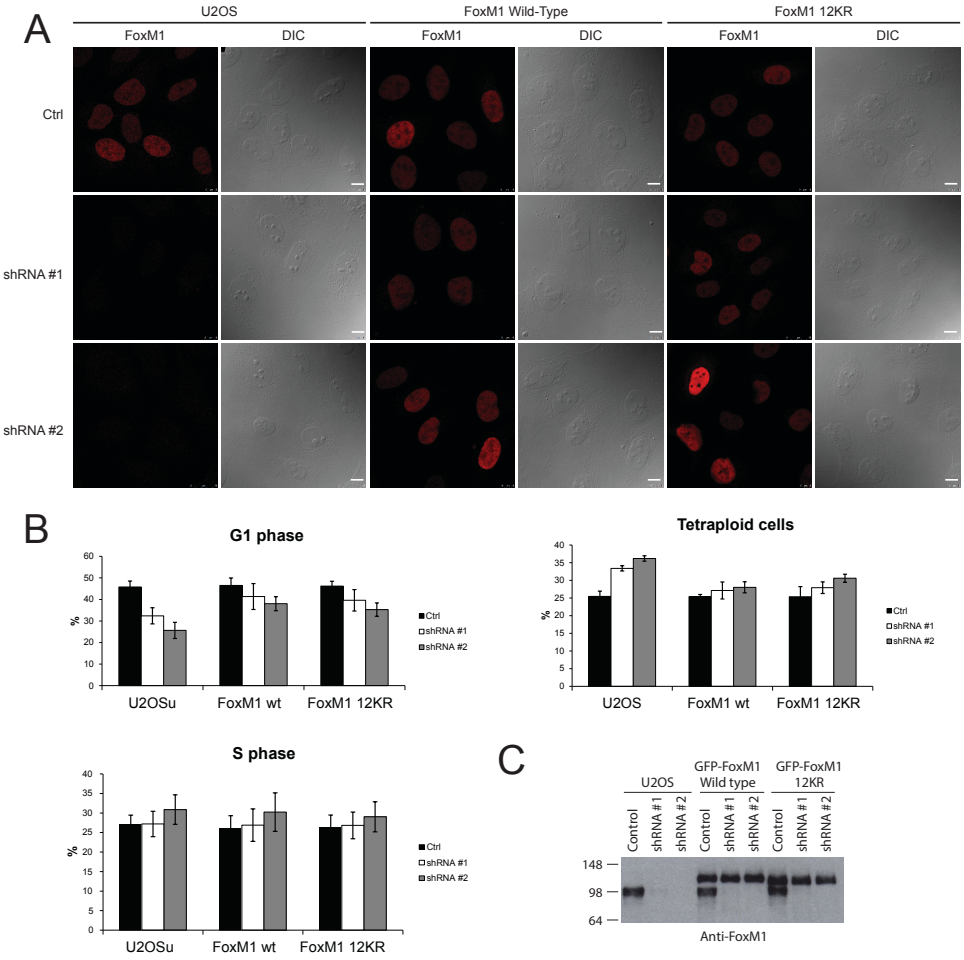

Figure S7. FoxM1 knockdown and complementation experiments.

A) U2OS cells, U2OS cells stably expressing Flag-FoxM1 wild type or Flag-FoxM1 12KR were infected with a non-targeting shRNA lentivirus, or two independent lentiviruses encoding FoxM1 shRNAs (shRNA #1 and #2). Cells were fixed three days after infection, stained with antibodies to detect FoxM1 and analyzed by confocal microscopy. Scale bars are 10 µM.

B) FACS analysis of G1 phase, S phase and tetraploid cells for the rescue experiment described in figures 7A and 7B. Average values from three independent experiments are shown in percentages; the error bars indicate the standard deviation from the average.

C) U2OS cells, U2OS cells stably expressing GFP-FoxM1 wild type or GFP-FoxM1 12KR were infected with a non-targeting shRNA lentivirus, or two independent lentiviruses encoding FoxM1 shRNAs (shRNA #1 and #2). Three days after infection cells were harvested for immunoblotting analysis with a FoxM1 antibody.

Supplemental Experimental Procedures

Plasmids

The mature protein that we refer to as SUMO-2-Q87R has the following amino acid sequence: MSEEKPKEGVKTENDHINLKVAGQDGSVVQFKIKRHTPLSKLMKAYCERQGLSMRQIRFRFDGQPINETDTPAQLEMEDEDTIDVFRQQTGG [1]. The open reading frame of this protein was amplified with the following primers: 5'-TTACTGCAGATGGACTACAAGGACGACGATGACAAGACTAGTATGTCCGAGGAGAAGCC-3' and 5'-AATCTCGAGCTAACCTCCCGTCTGCTGCCG-3' to introduce an N-terminal Flag-tag. This PCR product was cloned in between the *Pst*I and *Xho*I site of the plasmid pLV-CMV-IRES-eGFP [2] for lentiviral infection. The cDNA encoding the human FoxM1 protein was obtained from the Mammalian Gene Collection (MGC code 9577; Image ID 3881055; supplied by Source Bioscience) and amplified by a two-step PCR reaction using the following primers: 5'-AAAAAGCAGGCTTAATGAAAACTAGCCCCCGTCG-3' and 5'-A GAAAGCTGGGTTCTACTGTAGCTCAGGAATAAAC-3' for the first reaction and 5'-GGGGACAAGTTTGTACAAAAAAGCAGG CT-3' and 5'-GGGGACCACTTTGTACAAGAAAGCTGGGT-3' for the second reaction. The cDNA was inserted into pDON207 employing standard Gateway technology (Invitrogen). pDON207-FoxM1-12KR was generated by a gene synthesis service (GenScript). Silent mutations in both pDON207-FoxM1 wild type and pDON207-FoxM1-12KR were introduced by QuickChange site-directed mutagenesis (Stratagene) using oligonucleotides 5'-CTAAGAGATCCCCTGCACAGCAAGAATCCAACCAGGCAGAGGCCTCCAAG-3' and 5'-CTTGGAGGCCTCTGCCTGGTTGGATTCTTGCTGTGCAGGGGATCTCTTAG-3' for resistance to FoxM1 shRNA #1 and 5'-GTTTCTGGCCTTGCAGCAAACCGGTCCCTAACTGAGGGCCTGGTCCTG-3' and 5'-CAGGACCAGGCCCTCAGTTAGGGACCGGTTTGCTGCAAGGCCAGAAAC-3' for resistance to FoxM1 shRNA #2. To generate pDON207-FoxM1-4KR and 8KR we have swapped regions of the wild type and 12KR constructs by restriction of these plasmids with *Bss*SI and *Xcm*I and subsequent ligation. These cDNAs were subsequently transferred to multiple different destination vectors to generate T7-6His-FoxM1 expression constructs, HA-tagged FoxM1 expression plasmids (pMT2-HA-Dest, a kind gift of Drs. Petra de Graaf and Marc Timmers, Utrecht, The Netherlands) or GFP- tagged FoxM1 (pBabe-GFP-puro-DEST, also a kind gift of Drs. Petra de Graaf and Marc Timmers, Utrecht, The Netherlands). cDNA of FoxM1 wild type and FoxM1-12KR was cloned into the *Spe*I and *Xho*I cloning sites of a pLV-Flag-IRES-GFP construct using the following primers: 5'-TTAACTAGTATGAAAACTAGCCCCCG-3' and 5'-AATCTCGAGCTACTGTAGCTCAGGAATAAAC-3' to generate Flag-tagged, GFP sortable FoxM1 constructs. All fusions were made to the N-terminus of FoxM1. The cDNA encoding the mouse FoxM1 protein was obtained from the Mammalian Gene Collection (Image ID 6417437; supplied by Source Bioscience) and amplified by a two-step PCR reaction using the following primers: 5'-AAAAAGCAGGCTCGATGAGAACCAGCCCCCGCCG-3' and 5'-AGAAAGCTGGGTGCTAAGGGATGAACTGAGAC-3' for the first reaction and 5'-GGGGACAAGTTTGTACAAAAAAGCAGGCT-3' and 5'-GGGGACCACTTTGTACAAGAAAGCTGGGT-3' for the second reaction. The cDNA was inserted into pDON207 employing standard Gateway technology (Invitrogen). Mutations were introduced by QuickChange site-directed mutagenesis using the following oligonucleotides: 5'-CAGCGTTAAGCAGGCACTGGAAGAGAAG-3' and 5'-CTTCTCTTCCAGTGCCTGCTTAACGCTG-3' (E201A), 5'-CGGGTTAAGGTTGCGGAGCCCTCAGGAG-3' and 5'-CTCCTGAGGGCTCCGCAACCTTAACCCG-3' (E218A), 5'-CCATCAAAACTGCAATCCCACTGGG-3' and 5'-CCCAGTGGGATTGCAGTTTTGATGG-3' (E356A), 5'-CCATTAAGGAAGCAGAAATGCAGCCTG-3' and 5'-CAGGCTGCATTTCTGCTTCCTTAATGG-3' (E461A), 5'-CCTATCAAAGTGGCGAGCCCTCCCTTG-3' and 5'-CAAGGGAGGGCTCGCCACTTTGATAGG-3' (E479A), 5'-CGCTCAAAGAGGCGCTATCCAACTC-3' and 5'-GAGTTGGATAGCGCCTCTTTGAGCG-3' (E496A). Wild type and 6EA mouse FoxM1 cDNAs were subsequently transferred to the pcDNA3.1/nV5-DEST expression vector (Invitrogen). The 6x-FoxM1 DB-Luciferase, *CENP-F* promoter Luciferase and the GST tagged N terminal FoxM1 constructs were described previously [3, 4]. The CMV-LacZ reporter construct used in Luciferase assays was a kind gift of Dr. Erik Meulmeester. The SUMO-1 and SUMO-2 expressing constructs pE1E2S1 and pE1E2S2 were a kind gift of Dr. Hisato Saitoh [5].

Antibodies

The primary antibodies used were as followed: mouse anti-Ubc9 (BD Biosciences), mouse anti-UBA2

(Transduction Laboratories) mouse anti-Bromodeoxyuridine-Fluorescein (Roche Applied Science), mouse monoclonal anti-Flag M2, rabbit anti-HMGN5, mouse anti-polyHistidine Clone HIS-1 (All from Sigma), mouse monoclonal anti-SUMO-2/3 (Abcam), mouse anti-cJun and rabbit anti-ETV6 (kind gifts from Dr. D. Baker, Leiden, The Netherlands), rabbit anti-FoxP1 (Abcam), rabbit anti-FoxM1, mouse anti-Ubiquitin P4D1 (both from Santa Cruz Biotechnology), mouse monoclonal anti-HA.11 (Covance), mouse monoclonal anti-Methylated lysine (Abcam), mouse monoclonal anti-polyHistidine Clone HIS-1 (Sigma), rabbit anti-GTF21RD1, rabbit anti-JARID1B, rabbit anti-MDC1, rabbit anti-MYBL2, rabbit anti-SATB2, rabbit anti-RanBP2 (all from Bethyl laboratories), rabbit anti-MCM4 (Epitomics), mouse anti-RanGAP1 (Life Technologies), rabbit anti-V5 (Abcam), rabbit anti-SUMO-2/3 as previously described [6].

SILAC labeling

For SILAC labeling, cells were grown in medium supplemented with [$^{12}C_6$,$^{14}N_4$]arginine (referred to as R0), [$^{13}C_6$,$^{14}N_4$]arginine (referred to as R6), [$^{13}C_6$,$^{15}N_4$]arginine (referred to as R10), [$^{12}C_6$$^{14}N_2$]lysine (referred to as K0), [$^{2}H_4$,$^{12}C_6$,$^{14}N_2$]lysine (referred to as K4), or [$^{13}C_6$,$^{15}N_2$]lysine (referred to as K8) as indicated.

Lentiviral shRNA experiments

HeLa cells were infected at MOI 3 with lentivirus encoding shRNA TRCN0000007472 (shRNA1), shRNA TRCN0000007205 (shRNA2) or shRNA TRCN0000007206 (shRNA3). The medium was changed the next day and three days after infection, cells were transferred to different plates to proceed with FACS analysis, WST-1 analysis and colony formation assay. U2OS cells and U2OS cells stably expressing Flag-FoxM1 wild type or Flag-FoxM1 12KR were infected at MOI 2 with lentiviruses encoding shRNA TRCN 0000015544 (shRNA #1) or shRNA TRCN0000015546 (shRNA #2) against FoxM1. Cells were split one day after infection and processed three days after infection for FACS analysis, immunoblotting and microscopy. In all shRNA experiments, a non-targeting shRNA SHC002 was used as a control virus. All shRNA constructs belong to the Mission shRNA library from Sigma-Aldrich.

WST-1 analysis

On day three after lentivirus infection, cells were transferred (three wells per lentivirus construct in the first and second experiment, four wells per construct in the third experiment) to a 96-well plate at a density of 3000 cells per well. After another 24 hours, the old medium was removed and 100 µl of medium mixed 10:1 with WST-1 cell metabolic activity reagent (Roche) was added to each well. The absorbance at 450 nm was measured two hours after addition of the reagent in a micro-plate reader Victor 3 (Perkin Elmer).

Colony formation assay

For the colony formation assay, cells were transferred to 10 cm dishes on day three after the lentivirus infection at a density of 10,000 cells per dish. Colonies were grown until day nine after the infection and fixed with methanol and acetic acid (3:1) for 15 minutes at room temperature. After drying the dishes, colonies were stained with Giemsa solution (Merck). Colony formation was quantified using ImageJ Version 1.47v software.

Synchronization of cells

Cells were blocked with 4 mM thymidine (Sigma) for 16 hours or 10 µM RO-3306 (Calbiochem) for 20 hours and released from this blockage by washing two times with PBS and adding fresh DMEM. A single round of thymidine blocking was performed to limit DNA damage associated with this treatment. After the indicated time of release, cells were harvested by a mild trypsin treatment, one fifth of the sample was fixed for FACS analysis and the remaining sample was lysed in 4 pellet volumes of Flag-IP lysis buffer (1% SDS, 0.5% NP-40, 50 mM sodium fluoride, 1 mM sodium orthovanadate, 5 mM β-glycerol phosphate, 5 mM sodium pyrophosphate, 0.5 mM EGTA, 5 mM 1,10-phenanthroline, protease inhibitor including EDTA (Roche; 1 tablet per 10 ml buffer) in PBS). Lysates were frozen in

liquid nitrogen and, if needed, stored at -80°C.

Immunoprecipitation

Flag-IP lysates described above were thawed at 30°C and 70 mM chloroacetamide was added freshly. Samples were sonicated and incubated for 30 minutes at room temperature. Afterwards, samples were equalized using BCA and 30 µl of each lysate were kept as an input sample. An equal volume of dilution buffer (2% Triton X-100, 0.5% sodium deoxycholate, 1% BSA, freshly added 70 mM chloroacetamide, 5 mM sodium fluoride, 1 mM sodium orthovanadate, 5 mM β-glycerol phosphate, 5 mM sodium pyrophosphate, 0.5 mM EGTA, 5 mM 1,10-phenanthroline, protease inhibitor including EDTA (Roche; 1 tablet per 10 ml buffer) in 1x PBS) was added to the lysates and they were subsequently centrifuged for 45 minutes at 13.2 krpm at 4°C. The supernatant was mixed with prewashed Flag-M2 beads (Sigma; 30 µl beads per 1 ml of diluted sample) and incubated at 4°C for 90 minutes. Afterwards, the beads were washed 5 x with wash buffer (50 mM Tris, 150 mM NaCl, 70 mM chloroacetamide, 0.5% NP-40, 5 mM sodium fluoride, 1 mM sodium orthovanadate, 5 mM β-glycerol phosphate, 5 mM sodium pyrophosphate, 0.5 mM EGTA, 5 mM 1,10-phenanthroline, protease inhibitor including EDTA (Roche; 1 tablet per 10 ml buffer)) including three tube changes. Flag-SUMO-2 conjugates or Flag-FoxM1 proteins were eluted with one bead volume of 5% SDS and 1 mM Flag M2 epitope peptide in wash buffer. For SUMO-2/3 IPs, mouse monoclonal SUMO-2/3 antibodies were coupled to protein G sepharose (GE Healthcare). Cell lysis and the IP were performed as described above. SUMO-2/3 conjugates were eluted with one bead volume 1x NuPAGE LDS sample buffer (Invitrogen).

Fluorescence-activated cell sorting analysis and BrdU labeling

Cells were harvested by a mild trypsin treatment, washed two times with PBS and resuspended in 1.5 ml of PBS. Afterwards, 3.75 ml of 100% ethanol was added and the cells were fixed at 4°C at least overnight. On the day of flow cytometry analysis, the cells were first centrifuged at 1200 rpm for 2 minutes, the supernatant was removed and the cells were washed with PBS and 2% calf serum. Then, the cells were pelleted again and resuspended in 500 µl of PBS complemented with 2% calf serum, 25 µg/ml propidium iodide (Sigma) and 100 µg/ml RNase A (Sigma). Cellular DNA content was determined by flow cytometry with the BD LSRII system and BD FACS DIVA Software (BD Biosciences Clontech). Newly synthesized DNA was labeled by replacing the cell medium with medium containing 20 µM BrdU (Sigma). After 30 minutes of incorporation, the cells were released for 0, 4 or 8 hours. Cells were harvested by a mild trypsin treatment, washed once with PBS and resuspended in 0.5 ml of PBS. Subsequently, 5 ml of 70% ethanol was added and the cells were fixed at 4°C at least overnight. Next, the cells were washed with PBS and resuspended in 200 µl RNase A (0.5 mg/ml). After a 30 minute incubation at 37°C, the RNase A was removed by washing once with PBS. Afterwards, the cells were resuspended in 500 µl of solution A (5 M HCl and 0.5% Triton in MQ) and incubated for 20 minutes at room temperature. After neutralizing the solution by adding 10 ml of 1 M Tris pH 7.5, the cells were washed once with wash buffer 1 (0.5% Tween and 1% BSA in PBS). Subsequently, the cells were resuspended in FITC-conjugated anti-BrdU antibody (Roche) solution and incubated for 30 minutes at room temperature in the dark. Finally, the cells were washed twice with wash buffer 2 (0.5% Tween and 2% FCS in PBS), resuspended in PBS containing 20 µg/ml propidium iodide and analyzed by flow cytometry as described above.

Electrophoresis and immunoblotting

Protein samples were either separated via regular SDS-PAGE using a Tris-glycine buffer or on Novex 4-12% Bis-Tris gradient gels (Invitrogen) using MOPS buffer. Fractionated proteins were transferred onto Hybond-C extra membranes (Amersham Biosciences) using a submarine system (Invitrogen). Membranes were stained for total protein amounts with Ponceau S (Sigma) and blocked with PBS containing 5% milk powder and 0.1% Tween-20 before incubating with the primary antibodies as indicated.

Coomassie staining and in-gel digestion

Proteins were fractionated on Novex 4-12% gradient gels (Invitrogen) and stained with the Colloidal Blue Kit (Invitrogen) according to the manufacturer's protocol. Gel-lanes were divided into ten different slices as indicated and each slice was cut into 1 mm^3 cubes. Gel slices were de-stained with 50% ethanol in 25 mM ammonium bicarbonate solution and dehydrated with absolute ethanol. Proteins were digested with sequencing-grade modified trypsin (Sigma) overnight. Trypsin activity was quenched by acidification with TFA and peptides were extracted from the gel plugs with increasing concentrations of acetonitrile in 0.5% acetic acid. Organic solvent was evaporated in a vacuum centrifuge [7].

Mass Spectrometry Analysis

The resulting peptides from in-gel digestion were desalted and concentrated on STAGE-tips with two C18 filters and eluted two times with 10 µl 40% acetonitrile in 0.5% acetic acid prior to online nanoflow liquid chromatography-tandem mass spectrometry (nano LC-MS/MS). All the experiments were performed on an EASY-nLC system (Proxeon, Odense, Denmark) connected to the LTQ-Orbitrap Velos or to the Q-Exactive (both from Thermo Fisher Scientific, Germany) through a nano-electrospray ion source. Peptides were separated in a 15 cm analytical column in-house packed with either 1,9 or 3 µm C18 beads (Reprosil-AQ, Pur, Dr. Manish, Ammerbuch-Entringen, Germany) with a 80 minutes gradient from 8% to 75% acetonitrile in 0.5% acetic acid at a flow rate of 250 nl/minute. The mass spectrometers were operated in data-dependent acquisition mode with a top 10 method. For Q-Exactive measurements, full-scan MS spectra were acquired at a target value of 1 x 10^6 and a resolution of 70,000, and the Higher-Collisional Dissociation (HCD) tandem mass spectra (MS/MS) were recorded at a target value of 1 x 10^6 and with a resolution of 35,000 with a normalized collision energy of 25%. For LTQ-Orbitrap Velos measurements, full-scan MS spectra were acquired at a target value of 1 x 10^6 and a resolution of 30,000, and the Higher-Collisional Dissociation (HCD) tandem mass spectra (MS/MS) were recorded at a target value of 5 x 10^4 and with a resolution of 7,500 with a normalized collision energy of 35%.

Peptide and protein identification

Raw mass spectrometric (MS) files were processed with the MaxQuant software suite (version 1.4.0.3, Max Planck Institute of Biochemistry, Department of Proteomics and Signal Transduction, Munich, Germany) by which the precursor MS signal intensities were determined and SILAC triplets were automatically quantified. HCD-MS/MS spectra were deisotoped and filtered such that only the 10 most abundant fragments for each 100 mass/charge ratio (m/z) range were retained [8]. Proteins were identified by searching the HCD-MS/MS peak lists against a target/decoy version of the complete human Uniprot database supplemented with commonly observed contaminants such as porcine trypsin and bovine serum proteins. Tandem mass spectra were matched with an initial mass tolerance of 4.5 ppm on precursor masses and 20 ppm for fragment ions. Cysteine carbamidomethylation was searched as a fixed modification. Protein N-acetylation, N-pyroglutamine, oxidized methionine and SUMOylation (QQTGG) with monoisotopic mass of 471.20776 Da and pyroSUMOylation (pyroQQTGG) with monoisotopic mass of 454.18121 Da on lysine residues as variable modifications for the experiment. QQTGG and pyroQQTGG modified lysines were required to be located internally in the peptide sequence. Site localization probabilities were determined by MaxQuant using the PTM scoring algorithm [9, 10]. The data set was filtered by posterior error probability to achieve a false discovery rate (FDR) below 1%. Only peptides with Andromeda score > 25 (unmodified and modified) were included in the total peptide list. Protein/peptides were considered as SUMOylated if they had a SILAC ratio > 2 between the Flag-SUMO-2 cell line and the parental control cells.

Bioinformatics analysis

Protein interaction network analysis was performed using interaction data from the STRING database version 9.05 [11]. Only interactions with a STRING score above 0.4 are represented in the networks. Cytoscape (version 3.0.1) was used for visualization of protein interaction networks [12]. Clusters in that network were identified with MCODE (version 1.4.0 beta2) with MCODE score >6. MCODE is

a Cytoscape plugin that finds clusters (highly interconnected regions) in a network. Clusters mean different things in different types of networks. For instance, clusters in a protein-protein interaction network are often protein complexes and parts of pathways, while clusters in a protein similarity network represent protein families [13]. Proteins in MCODE clusters were color-coded according to their cell-cycle peak-time using the cell-cycle color-scheme method previously described [14]. Significantly enriched Gene Ontology annotation terms were determined using Fisher's exact test from InnateDB [15]. P values were corrected for multiple hypotheses testing using the Benjamini and Hochberg FDR.

Purification of His-SUMO and His-Ubiquitin conjugates

U2OS cells expressing His-SUMO-2 or His-Ubiquitin were washed and collected in ice-cold PBS. Small aliquots of cells were lysed in 1x LDS for input samples. Guanidine lysis buffer (6 M guanidine-HCl, 0.1 M Na_2HPO_4/NaH_2PO_4, 0.01 M Tris/HCl, pH 8.0 and competing imidazole) was added to the cell pellet to lyse the cells, after which the lysates were sonicated to reduce the viscosity. These lysates were used to determine the protein concentration using the BCA Protein Assay Reagent (Thermo Scientific); lysates were equalized and His-SUMO-2 or His-Ubiquitin conjugates were enriched on nickel-nitrilotriacetic acid-agarose beads (Qiagen) after which the beads were washed using wash buffers A to D. Wash buffer A: 6 M guanidine-HCl, 0.1 M Na_2HPO_4/NaH_2PO_4, 0.01 M Tris/HCl, pH 8.0, 10 mM β-mercaptoethanol, 0.3% Triton X-100. Wash buffer B: 8 M urea, 0.1 M Na_2HPO_4/NaH_2PO_4, 0.01 M Tris/HCl, pH 8.0, 10 mM β-mercaptoethanol, 0.3% Triton X-100. Wash buffer C: 8 M urea, 0.1 M Na_2HPO_4/NaH_2PO_4, 0.01 M Tris/HCl, pH 6.3, 10 mM β-mercaptoethanol, 0.3% Triton X-100. Wash buffer D: 8 M urea, 0.1 M Na_2HPO_4/NaH_2PO_4, 0.01 M Tris/HCl, pH 6.3, 10 mM β-mercaptoethanol, 0.1% Triton X-100. Samples were eluted in 7 M urea, 0.1 M Na_2HPO_4/NaH_2PO_4, 0.01 M Tris/HCl, pH 7.0, 500 mM imidazole.

Luciferase assays

U2OS cells were grown on 24-well tissue culture plates and co-transfected with 100 ng of the luciferase reporter construct, 100 ng of the LacZ reporter construct and 300 ng expression plasmid as indicated. 48 hours after transfection, cells were washed with ice-cold PBS and lysed in 100 µl of Reporter Lysis Buffer (Promega) for luciferase activity measurement or in SNTBS (2% SDS, 1% NP-40, 150 mM NaCl, 50 mM Tris pH 7.5) for immunoblotting. Experiments were carried out in quadruplicate and all values were corrected for β-gal activity.

RNA isolation, RT-PCR and quantitative PCR

Total RNA was purified from 6 cm dishes using the SV total RNA isolation system (Promega) according to the manufacturer's protocol. Total RNA was amplified and converted into double-stranded cDNA by reverse transcription using ImProm-II Reverse Transcriptase (Promega) and Random Hexamers (Invitrogen). Real-time quantitative PCR was performed using a CFX384 Touch Real-Time PCR detection system (Bio-Rad) in which PCR reactions were performed in a 10 µl volume containing cDNA, FastStart Universal SYBR Green Master mix (Roche) and specific primers. The PCR was carried out with an initial denaturation at 95°C for 3 minutes, followed by 40 cycles of 95°C for 20 seconds, 55°C annealing for 20 seconds and 60°C elongation for 30 seconds. The following sense (S) and antisense (AS) primer sequences were used: *Aurora kinase B*, S 5'-ATTGCTGACTTCGGCTGGT-3', AS 5'-GTCCAGGGTGCCACACAT-3', *Cyclin-B1*, S 5'-TTTCGCCTGAGCCTATTTTG-3', AS 5'-GCACATCCAGATGTTTCCATT-3', *CENP-F*, S 5'-GAGTCCTCCAAACCAACAGC-3', AS 5'-TCCGCTGAGCAACTTTGAC-3', *SAP30*, S 5'-CGAGCTGGATAAGAGCGCAA-3', AS 5'- TGGTCTGGTTGGTAGCTTGA-3', *CAPNS1*, S 5'-ATGGTTTTGGCATTGACACATG-3', AS 5'- GCTTGCCTGTGGTGTCGC-3'. Data were analyzed with the Bio-Rad CFX3 Manager software, average expression levels of triplicates were normalized for *CAPNS1* expression levels.

Recombinant proteins

His-FoxM1 recombinant proteins were purified essentially as described previously [16]. Briefly, BL21 cells were co-transformed with a His-FoxM1 expression construct and the SUMO-2 expression vector

pE1E2S2 or SUMO-1 expression vector pE1E2S1. Cells were grown to an OD600 of 0.6. Cells were then grown overnight at 24°C in the presence of 0.1 mM isopropyl-β-D-thiogalactopyranoside (IPTG), 20 mM HEPES pH 7.5, 1 mM $MgCl_2$ and 0,05% Glucose. Lysates were prepared and SUMOylated His-FoxM1 proteins were affinity-purified on Talon beads (BD Biosciences). 32 µg of SUMOylated His-FoxM1 protein was incubated with 0.7 µg of SENP2cd (BostonBiochem) at room temperature for 1 hour to remove the SUMO-2 moieties. GST tagged N-terminal FoxM1 was produced in *E. coli* and purified as described previously [1].

***In vitro* interaction assay**

GST-Nterm-FoxM1 protein fragments bound to Glutathione Sepharose (GE Healthcare) or beads only were incubated with 5 µg of His-FoxM1 proteins for 1 hour at 4°C in NETN buffer (150 mM NaCl, 1 mM EDTA, 20 mM Tris pH 8.0, 0.5% NP-40). After incubation, beads were washed 5 times in NETN buffer. Beads were eluted in NETN buffer in the presence of 20 mM Glutathione (Sigma) at room temperature. The bound and unbound proteins were analyzed by immunoblotting.

Microscopy

Cells were grown on microscopy coverslips and fixed with 3.7% formaldehyde in PBS for 15 minutes at room temperature. Afterwards, cells were permeabilized with 1% Triton X-100 in PBS for 15 minutes and washed twice with PBS and once with PBS plus 0.05% Tween (PBS-T). Slides were blocked with 0.5% blocking reagent (Roche) in 0.1 M Tris, pH7.5 and 0.15 M NaCl for 10 minutes and the primary antibody was added for one hour. Coverslips were washed five times with PBS-T and incubated with the secondary antibody for one hour. Again, the coverslips were washed five times with PBS-T and dehydrated washing once with 70%, once with 90% and once with 100% ethanol. After drying the cells, the coverslips were mounted onto a microscopy slide using Citifluor/DAPI solution (500 ng/ml) and samples were analyzed using a LEICA CTR6500 microscope.

Statistical Analysis

All the experiments have been performed at least in triplicate. Results shown are mean ± s.d and the p-value was calculated by Student's two tailed t-test.

Supplemental Reference List

1. Tatham, M. H. et al. (2001) Polymeric chains of SUMO-2 and SUMO-3 are conjugated to protein substrates by SAE1/SAE2 and Ubc9. *J. Biol. Chem.* 276, 35368-35374
2. Vellinga, J. et al. (2006) A system for efficient generation of adenovirus protein IX-producing helper cell lines. *J. Gene Med.* 8, 147-154
3. Laoukili, J. et al. (2005) FoxM1 is required for execution of the mitotic programme and chromosome stability. *Nat. Cell Biol.* 7, 126-136
4. Laoukili, J. et al. (2008) Activation of FoxM1 during G2 requires cyclin A/Cdk-dependent relief of autorepression by the FoxM1 N-terminal domain. *Mol. Cell Biol.* 28, 3076-3087
5. Uchimura, Y., Nakamura, M., Sugasawa, K., Nakao, M., and Saitoh, H. (2004) Overproduction of eukaryotic SUMO-1- and SUMO-2-conjugated proteins in Escherichia coli. *Anal. Biochem.* 331, 204-206
6. Vertegaal, A. C. et al. (2004) A proteomic study of SUMO-2 target proteins. *J. Biol. Chem.* 279, 33791-33798
7. Lundby, A., and Olsen, J. V. (2011) GeLCMS for in-depth protein characterization and advanced analysis of proteomes. *Methods Mol. Biol.* 753, 143-155
8. Cox, J. et al. (2011) Andromeda: a peptide search engine integrated into the MaxQuant environment. *J. Proteome. Res.* 10, 1794-1805

9. Cox, J., and Mann, M. (2008) MaxQuant enables high peptide identification rates, individualized p.p.b.-range mass accuracies and proteome-wide protein quantification. *Nat. Biotechnol.* 26, 1367-1372
10. Olsen, J. V. et al. (2006) Global, in vivo, and site-specific phosphorylation dynamics in signaling networks. *Cell* 127, 635-648
11. Szklarczyk, D. et al. (2011) The STRING database in 2011: functional interaction networks of proteins, globally integrated and scored. *Nucleic Acids Res.* 39, D561-D568
12. Smoot, M. E., Ono, K., Ruscheinski, J., Wang, P. L., and Ideker, T. (2011) Cytoscape 2.8: new features for data integration and network visualization. *Bioinformatics.* 27, 431-432
13. Bader, G. D., and Hogue, C. W. (2003) An automated method for finding molecular complexes in large protein interaction networks. *BMC. Bioinformatics.* 4, 2
14. Jensen, L. J., Jensen, T. S., de, L. U., Brunak, S., and Bork, P. (2006) Co-evolution of transcriptional and post-translational cell-cycle regulation. *Nature* 443, 594-597
15. Lynn, D. J. et al. (2008) InnateDB: facilitating systems-level analyses of the mammalian innate immune response. *Mol. Syst. Biol.* 4, 218
16. Schimmel, J. et al. (2010) Positively charged amino acids flanking a sumoylation consensus tetramer on the 110kDa tri-snRNP component SART1 enhance sumoylation efficiency. *J. Proteomics* 73, 1523-1534